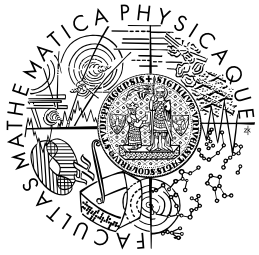

FACULTY
OF MATHEMATICS
AND PHYSICS
Charles University

**MASTER THESIS**

Martin Šípka

# Modeling of anisotropic viscoelastic fluids

Mathematical Institute of Charles University

. Supervisor of the master thesis: RNDr. Karel Tůma, Ph.D.

Study programme: Physics

Study branch: Mathematical and Computational Modelling in Physics

Prague 2020

I declare that I carried out this master thesis independently, and only with the cited sources, literature and other professional sources.

I understand that my work relates to the rights and obligations under the Act No. 121/2000 Sb., the Copyright Act, as amended, in particular the fact that the Charles University has the right to conclude a license agreement on the use of this work as a school work pursuant to Section 60 subsection 1 of the Copyright Act.

In ..... date .....  signature of the author

Firstly, I would like to express my deepest thanks to my supervisor RNDr. Karel Tůma, Ph.D and his colleagues for their help with perculiar problems I faced while writing this thesis. I would also like to thank my family and friends for their support.

Title: Modeling of anisotropic viscoelastic fluids

Author: Martin Šípka

Institute: Mathematical Institute of Charles University

Supervisor: RNDr. Karel Tůma, Ph.D., Mathematical Institute of Charles University

Abstract: In this thesis, we aim to create a framework for the derivation of thermodynamically consistent anisotropic viscoelastic models. As an example we propose simple models extending the isotropic Oldroyd-B and Giesekus models to illustrate the models' behavior and the process of finding the correct equations. We show what behavior in sheer we can expect and continue with a 3D simulation inspired by the experiment on a real liquid crystal mixture. Finally, we compare the simulation and the experiment to find similarities and possible further research topics.

Keywords: Viscoelastic fluids, second law of thermodynamics, rate of entropy production, anisotropy, liquid crystals.

Název práce: Modelování anizotropních viskoelastických tekutin

Autor: Martin Šípka

Ústav: Matematický ústav Univerzity Karlovy

Vedoucí diplomové práce: RNDr. Karel Tůma, Ph.D., Matematický ústav Univerzity Karlovy

Abstrakt: V této práci vytváříme základ pro odvození termodynamicky konzistentních anizotropních modelů. Jako příklad uvádíme jednoduché modely rozšiřující izotropní modely typu Oldroyd-B a Giesekus za účelem ilustrace jejich chování a postupu odvození správných rovnic. Ukážeme, jaké chování v jednoduchém smykovém proudění můžeme očekávat, a dále pokračujeme 3D simulací inspirovanou experimentem provedeným se směsí tekutých krystalů. Nakonec porovnáme simulaci s experimentem a pokusíme sa najít podobnosti a případná další témata hodná zkoumání.

Klíčová slova: Viskoelastické tekutiny, druhý zákon termodynamiky, rychlost produkce entropie, anizotropie, tekuté krystaly.

# Contents

# Introduction

Under the term fluid, one usually imagines quickly flowing streams of water or air. These are the typical cases of so-called Newtonian fluids whose viscosity is constant with respect to the stress or velocity of the fluid. However, there are many examples of non-Newtonian flows. Take for example something as solid as asphalt. It may seem to be hard at first but let it slowly flow for a long time and it behaves as a liquid [1]. Ice may be another such example. While it is definitely solid when we skate on it, it flows like a fluid if we examine it on timescales of millions of years. The viscosity of such fluids is no longer a constant. It may be dependent on various quantities such as time, the velocity of the flow, or the stress they are subjected to. Moreover, their response to deformation is often complicated. Their solid nature described for example by elasticity together with the aforementioned viscous behavior is why we call them viscoelastic.

Deriving rheological relations that are compatible with the second law of thermodynamics for such materials is a non-trivial challenge. In the past, the inspiration for the derivation of viscoelastic models was usually taken from springs and dashpots systems, connected so they formed an element with reasonable deformation response. These 1D mechanical systems were then generalized to 3D with the condition of maintaining the objectivity of the resulting relations. The generalization is not unique moreover, it was often unclear whether the entropy production is kept non-negative. Models extensively used in practice, such as an Oldroyd-B model [2] or a model by Giesekus [3], have been derived using this method.

In this thesis, the main goal is to extend the work done in the field of isotropic viscoelastic fluids that proposes an approach on how to consistently derive the constitutive equations directly employing the second law of thermodynamics. The so-called multiconfigurational approach was outlined in [4] and further developed for example in [5] and [6]. The models mentioned above, the Oldroyd-B or the Giesekus model can be derived using this approach [7]. The main advantage of the method is that we are not prescribing directly the stress tensor and all its degrees of freedom but rather just two scalar functions, the Helmholtz free energy describing elastic response and the dissipation giving us information about the viscous behavior. Since we employ the second law of thermodynamics directly, the models derived are consistently keeping the dissipation non-negative.

We seek to generalize this method by including anisotropy. Motivated by the article [8], which we aim to extend and update with recent progress in the theory, we shall develop a collection of useful relations that may be helpful in the future for anyone interested in the derivation of thermodynamically consistent anisotropic models. We also illustrate the method by providing examples of such models and simulations, describing briefly their behavior in simple geometries. The last section contains results from a three-dimensional experiment motivated by the real results for viscoelastic material, liquid crystals. While the focus of this work is on the general concepts and their illustrations, we, during the process discovered a rather interesting resemblance with much more elaborate and complex theories describing liquid crystals. By no means do we claim our model being any better for accurate descriptions than the models developed and tested

for more than fifty years now. However, we consider the similarity in behavior intriguing and worth further research. Among the effects observed during simulations is, for example, a parameter that influences tumbling or aligning behavior of the anisotropic fluid or the fact that the vector describing anisotropy rotates without any direct manipulation with nonsymmetric stress tensors.

# 1. Viscoelastic setting

## 1.1 Fundamentals

Continuum mechanics theory operates with the concept of deformation mapping and deformation gradient. When we consider the full deformation process, these quantities have an intuitive meaning and are introduced as a general concept to most students in the field of physics or engineering. We will be using the standard notation where deformation mapping is denoted $\chi(X,t)$ and deformation gradient $\mathbf{F}$. We will also need the other well-known concepts like material velocity $\mathbf{v}$ or density $\rho$. In purely viscous deformation we work with two configurations mapped by the deformation mapping. The reference configuration and the actual configuration.

### 1.1.1 Balance Laws

Below we summarise the balance equations in continuum mechanics. We list them in the simplest possible form including only the terms important for our further derivations. Before do so let us first start with a relation for the material time derivative for a scalar $\phi$, a vector $\mathbf{k}$ and a second order tensor $\mathbf{S}$.

$$\begin{aligned}\dot{\phi} &= \frac{\partial \phi}{\partial t} + \mathbf{v}\cdot\nabla\phi,\\ \dot{\mathbf{k}} &= \frac{\partial \mathbf{k}}{\partial t} + (\mathbf{v}\cdot\nabla)\mathbf{k},\\ \dot{\mathbf{S}} &= \frac{\partial \mathbf{S}}{\partial t} + (\mathbf{v}\cdot\nabla)\mathbf{S}.\end{aligned} \tag{1.1}$$

Now we can continue with the balance of mass that we will use in the standard form

$$\dot{\rho} = -\rho\,\mathrm{div}(\mathbf{v}). \tag{1.2}$$

Balance of linear momentum

$$\rho\dot{\mathbf{v}} = \mathrm{div}(\mathbf{T}) + \rho\mathbf{b}, \tag{1.3}$$

where $\mathbf{T}$ is the Cauchy stress tensor and $\mathbf{b}$ is a body force. We will further not consider any internal moment of inertia, giving us the balance of angular momentum in the simple form

$$\mathbf{T} = \mathbf{T}^T. \tag{1.4}$$

The balance of energy without considering energy production in the body of the fluid has the form

$$\rho\dot{\left(e + \frac{|v|^2}{2}\right)} = \mathrm{div}(\mathbf{T}\mathbf{v} - \mathbf{j}_e) + \rho\mathbf{b}\cdot\mathbf{v}, \tag{1.5}$$

Where $e$ is the internal energy, and $\mathbf{j}_e$ is the heat flux. After we substract the balance of linear momentum we get the equation for internal energy

$$\rho\dot{e} = \mathbf{T}\cdot\nabla\mathbf{v} - \mathrm{div}(\mathbf{j}_e). \tag{1.6}$$

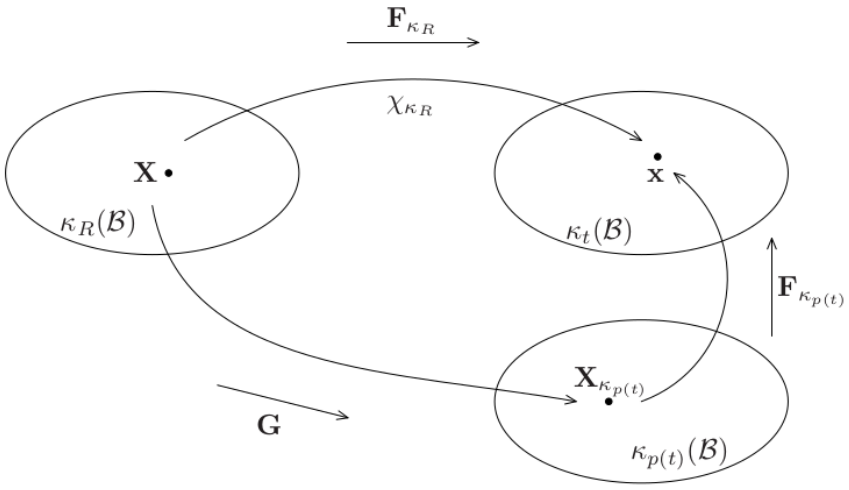


Figure 1.1: Scheme of the multiple configurations.

The last balance we need is the balance of entropy

$$\rho\dot{\eta} = -\operatorname{div}(\mathbf{j}_\eta) + \zeta, \tag{1.7}$$

where we introduced the entropy $\eta$, entropy flux $\mathbf{j}_\eta$ and entropy production $\zeta$. The second law of thermodynamics states that $\zeta \geq 0$.

## 1.2 Concept of natural configuration

Viscoelastic behavior can be described using the multiconfigurational approach. We consider the reference and actual configuration as before and all the quantities like deformation mapping and gradient remain the same. We, however, introduce the third configuration called the natural configuration and define a local mapping between reference and natural configuration as $\chi_{G(x)}$. We also define the mapping $\chi_{\kappa_{p(x)}}$ between natural and actual configuration. This allows us to work with viscous and elastic part of the deformation separately and bind them by their interaction so they form a closed system, the model of a viscoelastic fluid. Next, we will define the fundamental quantities necessary for the description of our multiconfigurational deformation.

### 1.2.1 Decomposition of the deformation gradient

All physics can be now derived from the simple relation that follows from the definition of mappings

$$\mathbf{F} = \mathbf{F}_{\kappa_{p(t)}}\mathbf{G}. \tag{1.8}$$

However, let us first define some kinematic quantities that will be used in the process. We define

$$\mathbf{C}_{\kappa_{p(t)}} = \mathbf{F}^T_{\kappa_{p(t)}}\mathbf{F}_{\kappa_{p(t)}} \text{ and } \mathbf{B}_{\kappa_{p(t)}} = \mathbf{F}_{\kappa_{p(t)}}\mathbf{F}^T_{\kappa_{p(t)}}, \tag{1.9}$$

as an elastic analogy to the standard right and left Cauchy-Green tensors $\mathbf{C}$ and $\mathbf{B}$. We also need an important quantity $\mathbf{L}_{\kappa_{p(t)}}$ insipred by the standard velocity

gradient $\mathbf{L} = \dot{\mathbf{F}}_{\kappa_{p(t)}}\mathbf{F}^{-1}_{\kappa_{p(t)}}$. We are going to define it as

$$\mathbf{L}_{\kappa_{p(t)}} = \dot{\mathbf{G}}\mathbf{G}^{-1}. \tag{1.10}$$

It will be useful in the next chapters to work with a decomposition of $\mathbf{L}_{\kappa_{p(t)}}$ in the form

$$\mathbf{L}_{\kappa_{p(t)}} = \mathbf{D}_{\kappa_{p(t)}} + \mathbf{W}_{\kappa_{p(t)}}. \tag{1.11}$$

Where $\mathbf{D}_{\kappa_{p(t)}}$ is the symmetric part and $\mathbf{W}_{\kappa_{p(t)}}$ skew-symmetric. We will also work with a polar decomposition of $\mathbf{F}_{\kappa_{p(t)}}$ in the form

$$\mathbf{F}_{\kappa_{p(t)}} = \mathbf{V}_{\kappa_{p(t)}}\mathbf{R}_{\kappa_{p(t)}}, \tag{1.12}$$

while it holds that

$$\mathbf{B}_{\kappa_{p(t)}} = \mathbf{F}_{\kappa_{p(t)}}\mathbf{F}^{T}_{\kappa_{p(t)}} = \mathbf{V}_{\kappa_{p(t)}}\mathbf{R}_{\kappa_{p(t)}}\mathbf{R}^{T}_{\kappa_{p(t)}}\mathbf{V}_{\kappa_{p(t)}} = \mathbf{V}^{2}_{\kappa_{p(t)}}, \tag{1.13}$$

since $\mathbf{R}_{\kappa_{p(t)}}$ is an orthogonal matrix. The next important step is finding the form of time derivatives of $\mathbf{F}_{\kappa_{p(t)}}$ and subsequently $\mathbf{B}_{\kappa_{p(t)}}$. Since from (1.8) $\mathbf{F}_{\kappa_{p(t)}} = \mathbf{F}\mathbf{G}^{-1}$ we can directly apply the material time derivative

$$\begin{aligned}\dot{\mathbf{F}}_{\kappa_{p(t)}} &= \overline{\mathbf{F}\dot{\mathbf{G}}^{-1}} = \dot{\mathbf{F}}\mathbf{G}^{-1} + \mathbf{F}\overline{\dot{\mathbf{G}}^{-1}} = \dot{\mathbf{F}}\mathbf{F}^{-1}\mathbf{F}\mathbf{G}^{-1} - \mathbf{F}\mathbf{G}^{-1}\dot{\mathbf{G}}\mathbf{G}^{-1} \\ &= \mathbf{L}\mathbf{F}_{\kappa_{p(t)}} - \mathbf{F}_{\kappa_{p(t)}}\mathbf{L}_{\kappa_{p(t)}}.\end{aligned} \tag{1.14}$$

This relation is central in a kinematic description of our viscoelastic fluid and allows us to further derive

$$\begin{aligned}\dot{\mathbf{B}}_{\kappa_{p(t)}} &= \dot{\mathbf{F}}_{\kappa_{p(t)}}\mathbf{F}^{T}_{\kappa_{p(t)}} + \mathbf{F}_{\kappa_{p(t)}}\dot{\mathbf{F}}^{T}_{\kappa_{p(t)}} \\ &= \mathbf{L}\mathbf{F}_{\kappa_{p(t)}}\mathbf{F}^{T}_{\kappa_{p(t)}} - \mathbf{F}_{\kappa_{p(t)}}\mathbf{L}_{\kappa_{p(t)}}\mathbf{F}^{T}_{\kappa_{p(t)}} + \mathbf{F}_{\kappa_{p(t)}}\mathbf{L}^{T}\mathbf{F}^{T}_{\kappa_{p(t)}} - \mathbf{F}_{\kappa_{p(t)}}\mathbf{L}^{T}_{\kappa_{p(t)}}\mathbf{F}^{T}_{\kappa_{p(t)}} \\ &= \mathbf{L}\mathbf{B}_{\kappa_{p(t)}} + \mathbf{B}_{\kappa_{p(t)}}\mathbf{L}^{T} - 2\mathbf{F}_{\kappa_{p(t)}}\mathbf{D}_{\kappa_{p(t)}}\mathbf{F}^{T}_{\kappa_{p(t)}}.\end{aligned} \tag{1.15}$$

Now from the definition of an upper convective Oldroyd derivative of a general tensor $\mathbf{S}$

$$\overset{\triangledown}{\mathbf{S}} = \dot{\mathbf{S}} - \mathbf{L}\mathbf{S} - \mathbf{S}\mathbf{L}^{T}, \tag{1.16}$$

we immediately get the relation for the upper convective derivative of tensor $\mathbf{B}_{\kappa_{p(t)}}$

$$\overset{\triangledown}{\mathbf{B}}_{\kappa_{p(t)}} = -2\mathbf{F}_{\kappa_{p(t)}}\mathbf{D}_{\kappa_{p(t)}}\mathbf{F}^{T}_{\kappa_{p(t)}}. \tag{1.17}$$

If we were concerned only with isotropic fludis, the quantities derived above would provide sufficient basis for our work. We however, being interested also with the interaction with rot-like structures, need also a way of describing the pure rotation that is a part of the deformation process. We will first look at the equation (1.14) and decompose the velocity gradient $\mathbf{L}_{\kappa_{p(t)}}$ into a symmetric and skew-symmetric part. The equation will change into

$$\dot{\mathbf{F}}_{\kappa_{p(t)}} = \mathbf{L}\mathbf{F}_{\kappa_{p(t)}} - \mathbf{F}_{\kappa_{p(t)}}\mathbf{D}_{\kappa_{p(t)}} - \mathbf{F}_{\kappa_{p(t)}}\mathbf{W}_{\kappa_{p(t)}}. \tag{1.18}$$

We will now multiply the equation with $\mathbf{F}^{T}_{\kappa_{p(t)}}$ from the right, so we will be able to use (1.17)

$$\begin{aligned}\dot{\mathbf{F}}_{\kappa_{p(t)}}\mathbf{F}^{T}_{\kappa_{p(t)}} &= \mathbf{L}\mathbf{F}_{\kappa_{p(t)}}\mathbf{F}^{T}_{\kappa_{p(t)}} - \mathbf{F}_{\kappa_{p(t)}}\mathbf{D}_{\kappa_{p(t)}}\mathbf{F}^{T}_{\kappa_{p(t)}} - \mathbf{F}_{\kappa_{p(t)}}\mathbf{W}_{\kappa_{p(t)}}\mathbf{F}^{T}_{\kappa_{p(t)}} \\ &= \mathbf{L}\mathbf{F}_{\kappa_{p(t)}}\mathbf{F}^{T}_{\kappa_{p(t)}} + \frac{1}{2}\overset{\triangledown}{\mathbf{B}}_{\kappa_{p(t)}} - \mathbf{F}_{\kappa_{p(t)}}\mathbf{W}_{\kappa_{p(t)}}\mathbf{F}^{T}_{\kappa_{p(t)}}.\end{aligned} \tag{1.19}$$

We are now interested in the expression for $\mathbf{F}_{\kappa_{p(t)}}\mathbf{W}_{\kappa_{p(t)}}\mathbf{F}^T_{\kappa_{p(t)}}$, since $\mathbf{W}_{\kappa_{p(t)}}$ will contain the information about $\mathbf{R}_{\kappa_{p(t)}}$. It will be important in order to correctly find the evolution equation for the direction of anisotropy.

$$\begin{aligned}\mathbf{F}_{\kappa_{p(t)}}\mathbf{W}_{\kappa_{p(t)}}\mathbf{F}^T_{\kappa_{p(t)}} &= -\dot{\mathbf{F}}_{\kappa_{p(t)}}\mathbf{F}^T_{\kappa_{p(t)}} + \mathbf{L}\mathbf{F}_{\kappa_{p(t)}}\mathbf{F}^T_{\kappa_{p(t)}} + \frac{1}{2}\overset{\triangledown}{\mathbf{B}}_{\kappa_{p(t)}} \\ &= -\dot{\mathbf{F}}_{\kappa_{p(t)}}\mathbf{F}^T_{\kappa_{p(t)}} + \mathbf{L}\mathbf{F}_{\kappa_{p(t)}}\mathbf{F}^T_{\kappa_{p(t)}} \\ &+ \frac{1}{2}\Big(\dot{\mathbf{B}}_{\kappa_{p(t)}} - \mathbf{L}\mathbf{B}_{\kappa_{p(t)}} - \mathbf{B}_{\kappa_{p(t)}}\mathbf{L}^T\Big).\end{aligned} \tag{1.20}$$

We simplify the equation

$$\mathbf{F}_{\kappa_{p(t)}}\mathbf{W}_{\kappa_{p(t)}}\mathbf{F}^T_{\kappa_{p(t)}} = \frac{1}{2}\mathbf{F}_{\kappa_{p(t)}}\dot{\mathbf{F}}^T_{\kappa_{p(t)}} - \frac{1}{2}\dot{\mathbf{F}}_{\kappa_{p(t)}}\mathbf{F}^T_{\kappa_{p(t)}} + \frac{1}{2}\mathbf{L}\mathbf{B}_{\kappa_{p(t)}} - \frac{1}{2}\mathbf{B}_{\kappa_{p(t)}}\mathbf{L}^T, \tag{1.21}$$

and use polar decomposition $\mathbf{F}_{\kappa_{p(t)}} = \mathbf{V}_{\kappa_{p(t)}}\mathbf{R}_{\kappa_{p(t)}}$

$$\begin{aligned}\mathbf{F}_{\kappa_{p(t)}}\mathbf{W}_{\kappa_{p(t)}}\mathbf{F}^T_{\kappa_{p(t)}} &= -\Big(\dot{\mathbf{V}}_{\kappa_{p(t)}}\mathbf{R}_{\kappa_{p(t)}} + \mathbf{V}_{\kappa_{p(t)}}\dot{\mathbf{R}}_{\kappa_{p(t)}}\Big)\mathbf{R}^T_{\kappa_{p(t)}}\mathbf{V}_{\kappa_{p(t)}} + \mathbf{L}\mathbf{B}_{\kappa_{p(t)}} \\ &+ \frac{1}{2}\Big(\dot{\mathbf{V}}_{\kappa_{p(t)}}\mathbf{V}_{\kappa_{p(t)}} + \mathbf{V}_{\kappa_{p(t)}}\dot{\mathbf{V}}_{\kappa_{p(t)}} - \mathbf{L}\mathbf{B}_{\kappa_{p(t)}} - \mathbf{B}_{\kappa_{p(t)}}\mathbf{L}^T\Big) \\ &= -\mathbf{V}_{\kappa_{p(t)}}\dot{\mathbf{R}}_{\kappa_{p(t)}}\mathbf{R}^T_{\kappa_{p(t)}}\mathbf{V}_{\kappa_{p(t)}} \\ &+ \frac{1}{2}\Big(\mathbf{V}_{\kappa_{p(t)}}\dot{\mathbf{V}}_{\kappa_{p(t)}} - \dot{\mathbf{V}}_{\kappa_{p(t)}}\mathbf{V}_{\kappa_{p(t)}} + \mathbf{L}\mathbf{B}_{\kappa_{p(t)}} - \mathbf{B}_{\kappa_{p(t)}}\mathbf{L}^T\Big).\end{aligned} \tag{1.22}$$

We may notice that the tensor $\dot{\mathbf{R}}_{\kappa_{p(t)}}\mathbf{R}^T_{\kappa_{p(t)}}$ is an skew-symmetric tensor commonly used when working with rigid body rotations. We will denote it

$$\boldsymbol{\Omega}_{\kappa_{p(t)}} = \dot{\mathbf{R}}_{\kappa_{p(t)}}\mathbf{R}^T_{\kappa_{p(t)}}. \tag{1.23}$$

The remaining terms will be denoted as

$$\mathbf{A}_{\mathbf{V}_{\kappa_{p(t)}}} = \frac{1}{2}\Big(\mathbf{V}_{\kappa_{p(t)}}\dot{\mathbf{V}}_{\kappa_{p(t)}} - \dot{\mathbf{V}}_{\kappa_{p(t)}}\mathbf{V}_{\kappa_{p(t)}} + \mathbf{L}\mathbf{B}_{\kappa_{p(t)}} - \mathbf{B}_{\kappa_{p(t)}}\mathbf{L}^T\Big). \tag{1.24}$$

So the final equation including the quantities that will be used from now on looks like

$$\mathbf{F}_{\kappa_{p(t)}}\mathbf{W}_{\kappa_{p(t)}}\mathbf{F}^T_{\kappa_{p(t)}} = -\mathbf{V}_{\kappa_{p(t)}}\boldsymbol{\Omega}_{\kappa_{p(t)}}\mathbf{V}_{\kappa_{p(t)}} + \mathbf{A}_{\mathbf{V}_{\kappa_{p(t)}}}. \tag{1.25}$$

## 1.3 Thermodynamics

In this thesis, we use thermodynamics as a tool for describing internal processes in the fluid and consider dissipation as a basis for finding constitutive relations for our model. We work with concepts such as thermodynamic potential or dissipation that are explained in detail for example in [9]. First, we will start with the definition of Helmholtz free energy $\psi$. We denote the internal energy $e$, temperature $\theta$ and entropy $\eta$. Let us point out that we will always be working with specific quantities. Helmholtz free energy is defined as follows

$$\psi = e - \theta\eta. \tag{1.26}$$

We differentiate in time

$$\dot{\psi} = \dot{e} - \dot{\theta}\eta - \theta\dot{\eta} \tag{1.27}$$

and multiply with density $\rho$

$$\rho\dot{\psi} = \rho\dot{e} - \rho\dot{\theta}\eta - \rho\theta\dot{\eta}. \tag{1.28}$$

Let us recall the inner ennergy balace

$$\rho\dot{e} = \mathbf{T} \cdot \mathbf{D} - \operatorname{div} \mathbf{j}_e \tag{1.29}$$

Where $\mathbf{T}$ is the Cauchy stress tensor and $\mathbf{D}$ the velocity gradient. Second term on the right side represents the energy flux. When we substitute in (1.28) we get

$$\rho\dot{\psi} = \mathbf{T} \cdot \mathbf{D} - \operatorname{div} \mathbf{j}_e - \rho\dot{\theta}\eta - \rho\theta\dot{\eta}. \tag{1.30}$$

Let us now introduce the second law of thermodynamics, bringing entropy production $\zeta$ in our equations

$$0 \leq \zeta = \rho\dot{\eta} + \operatorname{div} \mathbf{j}_\eta. \tag{1.31}$$

Now we can identify the term $\rho\dot{\eta}$ and get from the equation (1.30)

$$\rho\dot{\psi} = \mathbf{T} \cdot \mathbf{D} - \operatorname{div} \mathbf{j}_e - \rho\dot{\theta}\eta - \theta\zeta + \theta \operatorname{div} \mathbf{j}_\eta. \tag{1.32}$$

In this thesis we are going to assume isothermal process $\theta = const$ and also that $\theta\mathbf{j}_\eta = \mathbf{j}_e$. Since we work with the possitive dissipation this needs to be justified by either a large thermal capacity of the deformed body or a very high thermal conductivity and a thermal reservoir with a sufficient thermal capacity. Under this assumptions we may be able to consider the changes in the temperature neglectable. The isothermal process then results in the flux terms canceling out and naturally in $\dot{\theta} = 0$. We further define $\xi = \theta\zeta$ and require it to be non-negative. This simplifies the equation (1.32) to the form commonly known as the reduced thermodynamic identity

$$0 \leq \xi = \mathbf{T} \cdot \mathbf{D} - \rho\dot{\psi}. \tag{1.33}$$

Inequality, we just derived, is the condition we are aiming to meet for any model present in this thesis. We will be seeking a preferably simple form of dissipation $\xi$ while keeping $\xi$ possitive at all times.

### 1.3.1 Helmholtz free energy

One of the two places where there is a possible variation in the equations we will present is the Helmholtz free energy $\psi$. The reader interested in how different free energies can lead to various models is referred to for example [5]. In the isotropy setting we are going to work only with the free energy in the form

$$\psi = \frac{\mu}{2\rho}\Big( \operatorname{tr} \mathbf{B}_{\kappa_{p(t)}} - 3 - \ln \det(\mathbf{B}_{\kappa_{p(t)}})\Big), \tag{1.34}$$

motivated by [7]. The introduced constant $\mu$ is called the elastic modulus an is possitive. Notice that since $\mathbf{B}_{\kappa_{p(t)}}$ describes purely elastic deformation, the free

energy is stored only in this particular part of the deformation. Knowing $\psi$, we can now differentiate in time. We will apply the material time derivative to the term $\operatorname{tr}\mathbf{B}_{\kappa_{p(t)}}$.

$$\operatorname{tr}\dot{\mathbf{B}}_{\kappa_{p(t)}} = \operatorname{tr}\Big(\mathbf{L}\mathbf{B}_{\kappa_{p(t)}} + \mathbf{B}_{\kappa_{p(t)}}\mathbf{L} - 2\mathbf{F}_{\kappa_{p(t)}}\mathbf{D}_{\kappa_{p(t)}}\mathbf{F}^T_{\kappa_{p(t)}}\Big), \tag{1.35}$$

Which can be in coordinates rewritten as

$$\operatorname{tr}\dot{\mathbf{B}}_{\kappa_{p(t)}} = \mathbf{L}_{ij}(\mathbf{B}_{\kappa_{p(t)}})_{ji} + (\mathbf{B}_{\kappa_{p(t)}})_{ij}\mathbf{L}^T_{ji} - 2(\mathbf{F}_{\kappa_{p(t)}})_{ij}(\mathbf{D}_{\kappa_{p(t)}})_{jk}(\mathbf{F}^T_{\kappa_{p(t)}})_{ki}. \tag{1.36}$$

First two terms can be rearanged

$$\mathbf{L}_{ij}(\mathbf{B}_{\kappa_{p(t)}})_{ji} + \mathbf{L}_{ij}(\mathbf{B}_{\kappa_{p(t)}})_{ji} = 2\mathbf{B}_{\kappa_{p(t)}} \cdot \mathbf{L} = 2\mathbf{B}_{\kappa_{p(t)}} \cdot \mathbf{D}, \tag{1.37}$$

where we used the symmetry of the tensor $\mathbf{B}_{\kappa_{p(t)}}$ and the fact that a dot product of a symmetric and a skew-symmetric tensor is zero. The last term is

$$\begin{aligned} -2(\mathbf{F}_{\kappa_{p(t)}})_{ij}(\mathbf{D}_{\kappa_{p(t)}})_{jk}(\mathbf{F}^T_{\kappa_{p(t)}})_{ki} &= -2(\mathbf{F}^T_{\kappa_{p(t)}})_{ji}(\mathbf{F}_{\kappa_{p(t)}})_{ik} \cdot (\mathbf{D}_{\kappa_{p(t)}})_{jk} \\ &= -2\mathbf{C}_{\kappa_{p(t)}} \cdot \mathbf{D}_{\kappa_{p(t)}}. \end{aligned} \tag{1.38}$$

One gets

$$\operatorname{tr}\dot{\mathbf{B}}_{\kappa_{p(t)}} = 2\mathbf{B}_{\kappa_{p(t)}} \cdot \mathbf{D} - 2\mathbf{C}_{\kappa_{p(t)}} \cdot \mathbf{D}_{\kappa_{p(t)}}. \tag{1.39}$$

Let us now look at $\dot{\overline{\ln\det\mathbf{B}_{\kappa_{p(t)}}}}$ We will need the following relation

$$\dot{\overline{\det\mathbf{A}}} = \det(\mathbf{A})\operatorname{tr}(\dot{\mathbf{A}}\mathbf{A}^{-1}). \tag{1.40}$$

Then we can derive

$$\begin{aligned} \dot{\overline{\ln\det\mathbf{B}_{\kappa_{p(t)}}}} &= \frac{1}{\det(\mathbf{B}_{\kappa_{p(t)}})}\det(\mathbf{B}_{\kappa_{p(t)}})\operatorname{Tr}(\dot{\mathbf{B}}_{\kappa_{p(t)}}\mathbf{B}^{-1}_{\kappa_{p(t)}}) \\ &= \mathbf{L}\mathbf{B}_{\kappa_{p(t)}} \cdot \mathbf{B}^{-1}_{\kappa_{p(t)}} + \mathbf{B}_{\kappa_{p(t)}}\mathbf{L}^T \cdot \mathbf{B}^{-1}_{\kappa_{p(t)}} \\ &- 2\mathbf{F}_{\kappa_{p(t)}}\mathbf{D}_{\kappa_{p(t)}}\mathbf{F}^T_{\kappa_{p(t)}} \cdot \mathbf{B}^{-1}_{\kappa_{p(t)}} \end{aligned} \tag{1.41}$$

In index notation

$$\begin{aligned} &\mathbf{L}_{ij}(\mathbf{B}_{\kappa_{\mathbf{p(t)}}})_{jk}(\mathbf{B}^{-1}_{\kappa_{p(t)}})_{ki} + (\mathbf{B}_{\kappa_{p(t)}})_{ij}\mathbf{L}^T_{jk}(\mathbf{B}^{-1}_{\kappa_{p(t)}})_{ki} \\ &\quad - 2(\mathbf{F}_{\kappa_{p(t)}})_{ij}(\mathbf{D}_{\kappa_{p(t)}})_{jk}(\mathbf{F}^T_{\kappa_{p(t)}})_{kl} \cdot (\mathbf{B}^{-1}_{\kappa_{p(t)}})_{li} \\ &\quad = \mathbf{L}_{ij}\mathbf{I}_{ji} + \mathbf{L}^T_{ij}\mathbf{I}_{ji} - 2(\mathbf{D}_{\kappa_{p(t)}})_{ij}\mathbf{I}_{ji} \end{aligned} \tag{1.42}$$

so at the end

$$\dot{\overline{\ln\det\mathbf{B}_{\kappa_{p(t)}}}} = 2\mathbf{I} \cdot \mathbf{D} - 2\mathbf{I} \cdot \mathbf{D}_{\kappa_{p(t)}}. \tag{1.43}$$

The proper proof is done in [7].

### 1.3.2 Oldroyd-B model

We now have everything prepared for the derivation of the isotropic Oldroyd-B model that will serve as a basis for which we are seeking an anisotropic extension. let us write the resulting form of $\rho\dot{\psi}$

$$\begin{aligned} \rho\dot{\psi} &= \rho\frac{\mu}{2\rho}\Big(2\mathbf{B}_{\kappa_{p(t)}} \cdot \mathbf{D} - 2\mathbf{C}_{\kappa_{p(t)}} \cdot \mathbf{D}_{\kappa_{p(t)}} - \mathbf{I} \cdot \mathbf{D} + 2\mathbf{I} \cdot \mathbf{D}_{\kappa_{p(t)}}\Big) \\ &= \mu\Big(\mathbf{B}_{\kappa_{p(t)}} \cdot \mathbf{D} - \mathbf{C}_{\kappa_{p(t)}} \cdot \mathbf{D}_{\kappa_{p(t)}} - \mathbf{I} \cdot \mathbf{D} + \mathbf{I} \cdot \mathbf{D}_{\kappa_{p(t)}}\Big). \end{aligned} \tag{1.44}$$

Note that $\dot{\rho} = -\rho \operatorname{div}(\mathbf{v}) = 0$. Therefore the dissipation $\xi$ is

$$\begin{aligned}\xi &= \mathbf{T}\cdot\mathbf{D} - \mu\Big(\mathbf{B}_{\kappa_{p(t)}}\cdot\mathbf{D} - \mathbf{C}_{\kappa_{p(t)}}\cdot\mathbf{D}_{\kappa_{p(t)}} - \mathbf{I}\cdot\mathbf{D} + \mathbf{I}\cdot\mathbf{D}_{\kappa_{p(t)}}\Big)\\ &= \Big(\mathbf{T} - \mu(\mathbf{B}_{\kappa_{p(t)}} - \mathbf{I})\Big)^d\cdot\mathbf{D}^d + \Big(\mathbf{C}_{\kappa_{p(t)}} - \mathbf{I}\Big)\cdot\mathbf{D}_{\kappa_{p(t)}}\end{aligned} \tag{1.45}$$

We now arrive at the point where we can again choose the aprroach we will use. As we mentioned we require the dissipation to be possitive. There are, however, various approaches on how to get the most appropriate form. One possibility is the maximization of entropy production decribed in for example [10]. This process is rather complicated therefore we choose to simply prescribe closures that are linear. This will prove to be a reasonable decision as the dissipation will get more complex in the anisotropic setting. The dissipation we have to choose in order to get the Oldroyd-B model is

$$\xi = 2\nu\,|\mathbf{D}|^2 + 2\nu_1\mathbf{D}_{\kappa_{p(t)}}\mathbf{C}_{\kappa_{p(t)}}\cdot\mathbf{D}_{\kappa_{p(t)}},\ \ \nu,\nu_1 > 0. \tag{1.46}$$

This leads us to the constitutive equation for the stress tensor

$$\mathbf{T}^d - \mu(\mathbf{B}_{\kappa_{p(t)}} - \mathbf{I})^d = 2\nu\mathbf{D}^d, \tag{1.47}$$

from which $\mathbf{T}$ is simply

$$\mathbf{T}^d = 2\nu\mathbf{D}^d + \mu(\mathbf{B}_{\kappa_{p(t)}} - \mathbf{I})^d. \tag{1.48}$$

It is now important that we work with incompressible fluid. This means that $\operatorname{div}\mathbf{v} = 0$ and $\operatorname{tr}\mathbf{B}_{\kappa_{p(t)}} = 1$. Therefore $\mathbf{D}^d = \mathbf{D}$ and $(\mathbf{B}_{\kappa_{p(t)}} - \mathbf{I}) = \mathbf{B}^d_{\kappa_{p(t)}}$. We may simplify

$$\mathbf{T}^d = 2\nu\mathbf{D} + \mu\mathbf{B}^d_{\kappa_{p(t)}} \tag{1.49}$$

The equation for $\mathbf{B}_{\kappa_{p(t)}}$ will need a little extra work

$$\Big(\mathbf{C}_{\kappa_{p(t)}} - \mathbf{I}\Big) = 2\nu_1\mathbf{C}_{\kappa_{p(t)}}\mathbf{D}_{\kappa_{p(t)}}. \tag{1.50}$$

Multiplying by $\mathbf{F}^{-T}_{\kappa_{p(t)}}$ from the left and $\mathbf{F}^{T}_{\kappa_{p(t)}}$ from the right we arrive at

$$\Big(\mathbf{B}_{\kappa_{p(t)}} - \mathbf{I}\Big) = 2\nu_1\mathbf{F}_{\kappa_{p(t)}}\mathbf{D}_{\kappa_{p(t)}}\mathbf{F}^T_{\kappa_{p(t)}}. \tag{1.51}$$

Using (1.17) gives us

$$\Big(\mathbf{B}_{\kappa_{p(t)}} - \mathbf{I}\Big) + \nu_1\overset{\triangledown}{\mathbf{B}}_{\kappa_{p(t)}} = \mathbf{0}. \tag{1.52}$$

To summarize the equations

$$\begin{aligned}\operatorname{div}\mathbf{v} &= 0,\\ \rho\dot{\mathbf{v}} &= -\operatorname{div}\mathbf{T},\\ \mathbf{T} &= -p\mathbf{I} + 2\nu\mathbf{D} + \mu\mathbf{B}^d_{\kappa_{p(t)}}\\ \mu\Big(\mathbf{B}_{\kappa_{p(t)}} - \mathbf{I}\Big) &+ \nu_1\overset{\triangledown}{\mathbf{B}}_{\kappa_{p(t)}} = \mathbf{0}.\end{aligned} \tag{1.53}$$

### 1.3.3 Giesekus model

With only a slight modification of the closures we can arrive to a constitutive relation nonlinear in $\mathbf{B}_{\kappa_{p(t)}}$. The closures and therefore the dissipation we will use are

$$\xi = 2\nu \left|\mathbf{D}\right|^2 + 2\nu_1 \left|\mathbf{D}_{\kappa_{p(t)}}\right|^2, \ \nu, \nu_1 > 0. \tag{1.54}$$

This results in an equation for the Cauchy stress tensor is as before in the form

$$\mathbf{T}^d = 2\nu\mathbf{D} + \mu\mathbf{B}^d_{\kappa_{p(t)}}. \tag{1.55}$$

However, we need to modify the evolution equation for $\mathbf{B}_{\kappa_{p(t)}}$. We start with

$$\left(\mathbf{C}_{\kappa_{p(t)}} - \mathbf{I}\right) = 2\nu_1\mathbf{D}_{\kappa_{p(t)}}. \tag{1.56}$$

Now we multiply with $\mathbf{F}_{\kappa_{p(t)}}$ from the left and $\mathbf{F}^T_{\kappa_{p(t)}}$ from the right getting

$$\left(\mathbf{F}_{\kappa_{p(t)}}\mathbf{C}_{\kappa_{p(t)}}\mathbf{F}^T_{\kappa_{p(t)}} - \mathbf{B}_{\kappa_{p(t)}}\right) = 2\nu_1\mathbf{F}_{\kappa_{p(t)}}\mathbf{D}_{\kappa_{p(t)}}\mathbf{F}^T_{\kappa_{p(t)}}. \tag{1.57}$$

Which leads to

$$\mu\mathbf{B}_{\kappa_{p(t)}}\left(\mathbf{B}_{\kappa_{p(t)}} - \mathbf{I}\right) + \nu_1\overset{\triangledown}{\mathbf{B}}_{\kappa_{p(t)}} = \mathbf{0}. \tag{1.58}$$

We summarize

$$\begin{aligned} \operatorname{div}\mathbf{v} &= 0, \\ \rho\dot{\mathbf{v}} &= \operatorname{div}\mathbf{T} \\ \mathbf{T} &= -p\mathbf{I} + 2\nu\mathbf{D} + \mu\mathbf{B}^d_{\kappa_{p(t)}} \\ \mu\mathbf{B}_{\kappa_{p(t)}}\left(\mathbf{B}_{\kappa_{p(t)}} - \mathbf{I}\right) &+ \nu_1\overset{\triangledown}{\mathbf{B}}_{\kappa_{p(t)}} = \mathbf{0}. \end{aligned} \tag{1.59}$$

Now having our isotropic models, we can move on to the anisotropy. The goal is to compare the isotropic and anisotropic models later in the thesis.

# 2. Anisotropy

Our key assumption we will use in the entire chapter is

$$\dot{\mathbf{N}} = \mathbf{0}, \tag{2.1}$$

where $\mathbf{N}$ is the vector characterising anisotropy in the natural configuration. Next we assume the vector $\mathbf{n}$ in the actual configuration is related to $\mathbf{N}$ as

$$\mathbf{n} = \mathbf{F}_{\kappa_{p(t)}}\mathbf{N}. \tag{2.2}$$

We therefore get the following equation for the material time derivative.

$$\dot{\mathbf{n}} = \dot{\mathbf{F}}_{\kappa_{p(t)}}\mathbf{N}. \tag{2.3}$$

And knowing $\dot{\mathbf{F}}_{\kappa_{p(t)}}$ from (1.14) we can write

$$\dot{\mathbf{n}} = \mathbf{L}\mathbf{F}_{\kappa_{p(t)}}\mathbf{N} - \mathbf{F}_{\kappa_{p(t)}}\mathbf{L}_{\kappa_{p(t)}}\mathbf{N}. \tag{2.4}$$

This is now enough to derive neccessary kinematic equalities.

## 2.1 Kinematics

We start by one more decomposition. We introduce

$$\mathbf{n}^* = \mathbf{R}_{\kappa_{p(t)}}\mathbf{N}, \tag{2.5}$$

where $\mathbf{R}_{\kappa_{p(t)}}$ is the rotational part of the $\mathbf{F}_{\kappa_{p(t)}}$ as mentioned in (1.12). This gives us the purely rotated vector $\mathbf{n}^*$ that has the same length as vector $\mathbf{N}$. It may be natural to think of the vector field $\mathbf{N}$ as of the field of unit vectors leaving us with $|\mathbf{n}^*| = 1$. Let us look at the evolution equation for $\mathbf{n}^*$.

$$\dot{\mathbf{n}}^* = \dot{\mathbf{R}}_{\kappa_{p(t)}}\mathbf{N} = \dot{\mathbf{R}}_{\kappa_{p(t)}}\mathbf{R}^{-1}_{\kappa_{p(t)}}\mathbf{n}^* = \mathbf{\Omega}_{\kappa_{p(t)}}\mathbf{n}^*. \tag{2.6}$$

We may notice that the tensor $\mathbf{\Omega}_{\kappa_{p(t)}}$ is the same tensor as in (1.25). Once we know $\mathbf{n}^*$ we can get $\mathbf{n}$ as

$$\mathbf{n} = \mathbf{V}_{\kappa_{p(t)}}\mathbf{n}^*. \tag{2.7}$$

All three components of $\mathbf{n}$ are determined by knowing $\mathbf{B}_{\kappa_{p(t)}}$ and $\mathbf{n}^*$. Tensor $\mathbf{B}_{\kappa_{p(t)}}$ is calculated in the isotropic setting. Therefore, we may expect that the equation for anisotropy added in the process of enforcing positive entropy production will describe only $\mathbf{n}^*$. Since the vector $\mathbf{n}^*$ is a unit vector, we need to be careful with the number of equations added. We are only allowed to prescribe two independent equations. Deriving an equation for $\mathbf{n}$ directly from thermodynamics and constructing it in a similar way as we constructed an equation for $\mathbf{B}_{\kappa_{p(t)}}$ has proven to be a wrong approach. This way we prescribe a constitutive relation for three degrees of freedom for $\mathbf{n}$ when in fact, we could only prescribe two. There are two options on how to consistently approach the derivation of the evolution equation for $\mathbf{n}$. One is to derive the evolution equation for $\mathbf{F}_{\kappa_{p(t)}}$ and then subsequently construct two equations by appropriate manipulation. Another way, which we will follow, that allows more flexibility when choosing the closures is to consider closures in both $\mathbf{D}_{\kappa_{p(t)}}$ and $\mathbf{W}_{\kappa_{p(t)}}$. Since $\mathbf{W}_{\kappa_{p(t)}}$ is skew-symmetric, it will allow us to prescribe correctly the number of degrees of freedom. Moreover, we can in some way control how anisotropy influences the model by giving weights to entropy production in symmetric or skew-symmetric deformation.

## 2.2 Free energy of anisotropic fluid

We require our Helmholtz free energy to be composed of two separate terms. First term will be the free energy of the isotropic part dependent only on $\mathbf{B}_{\kappa_{p(t)}}$ and the second term representing the anisotropic part will depend solely on $\mathbf{n}$, i.e.

$$\psi = \psi_1(\mathbf{B}_{\kappa_{p(t)}}) + \psi_2(\mathbf{n}). \tag{2.8}$$

The isotropic part remains the same as in the previous chapter. Let us recall

$$\psi_1 = \frac{\mu}{2\rho}\Big(\operatorname{tr}\mathbf{B}_{\kappa_{p(t)}} - 3 - \ln\det(\mathbf{B}_{\kappa_{p(t)}})\Big). \tag{2.9}$$

There will, however, be a possible variance in the second term. In this thesis we are going to assume

$$\psi_2(\mathbf{n}) = \psi(|\mathbf{n}|^2, \mathbf{n}\mathbf{B}_{\kappa_{p(t)}}\cdot\mathbf{n}, \mathbf{n}\mathbf{B}^2_{\kappa_{p(t)}}\cdot\mathbf{n}, \dots, \mathbf{n}\mathbf{B}^n_{\kappa_{p(t)}}\cdot\mathbf{n}). \tag{2.10}$$

While in the proper transversly isotropic solid this is the only possible form of free energy, in the case of our anisotropic fluid that has no single direction of transversal anisotropy, free energy can be much more complicated. If we for example were to describe certain nematic liquid crystals, we would most likely need to include the energy dependence on the $\nabla\mathbf{n}$. The energy we will be using is in the form

$$\psi_2 = \frac{c_1}{2\rho}\Big(|\mathbf{n}|^2 - 1 - \ln(|\mathbf{n}|^2)\Big). \tag{2.11}$$

Let us now focus on the dissipation for a material with this particular free energy.

## 2.3 Anisotropic dissipation

Since we already know $\dot{\psi}_1$ from (1.44), we only need to calculate $\dot{\psi}_2$ and sum the results. We proceed by calculating

$$\rho\dot{\psi}_2 = \frac{c}{2}\Big(\dot{\overline{|\mathbf{n}|^2}} - \dot{\overline{\ln(|\mathbf{n}|^2)}}\Big). \tag{2.12}$$

Now, let us calculate the first one

$$\begin{aligned}\dot{\overline{\mathbf{n}^2}} &= 2\mathbf{n}\cdot\dot{\mathbf{n}} = 2\mathbf{n}\cdot\Big(\mathbf{L}\mathbf{F}_{\kappa_{p(t)}} - \mathbf{F}_{\kappa_{p(t)}}\mathbf{L}_{\kappa_{p(t)}}\Big)\mathbf{N}\\ &= 2\mathbf{N}\cdot\mathbf{F}^T_{\kappa_{p(t)}}\mathbf{L}\mathbf{F}_{\kappa_{p(t)}}\mathbf{N} - 2\mathbf{N}\cdot\mathbf{F}^T_{\kappa_{p(t)}}\mathbf{F}_{\kappa_{p(t)}}\mathbf{L}_{\kappa_{p(t)}}\mathbf{N}.\end{aligned} \tag{2.13}$$

Note that since $\mathbf{N}\cdot\mathbf{F}^T_{\kappa_{p(t)}}\mathbf{L}\mathbf{F}_{\kappa_{p(t)}}\mathbf{N} = \Big(\mathbf{F}_{\kappa_{p(t)}}\mathbf{N}\otimes\mathbf{F}_{\kappa_{p(t)}}\mathbf{N}\Big)\cdot\mathbf{L}$, it is in fact the scalar product of a symmetric tensor with $\mathbf{L}$. Therefore, skew-symmetric part of $\mathbf{L}$ has no contribution to the result and it holds

$$\mathbf{N}\cdot\mathbf{F}^T_{\kappa_{p(t)}}\mathbf{L}\mathbf{F}_{\kappa_{p(t)}}\mathbf{N} = \mathbf{N}\cdot\mathbf{F}^T_{\kappa_{p(t)}}\mathbf{D}\mathbf{F}_{\kappa_{p(t)}}\mathbf{N}. \tag{2.14}$$

The second term is similarly

$$\dot{\overline{\ln(|\mathbf{n}|^2)}} = \frac{2}{|\mathbf{n}|^2}\dot{\overline{|\mathbf{n}|^2}} = \frac{2}{|\mathbf{n}|^2}\Big(\mathbf{N}\cdot\mathbf{F}^T_{\kappa_{p(t)}}\mathbf{D}\mathbf{F}_{\kappa_{p(t)}}\mathbf{N} - \mathbf{N}\cdot\mathbf{F}^T_{\kappa_{p(t)}}\mathbf{F}_{\kappa_{p(t)}}\mathbf{L}_{\kappa_{p(t)}}\mathbf{N}\Big). \tag{2.15}$$

Therefore the final $\dot{\psi}_2$

$$\rho\dot{\psi}_2 = c\Big(1-\frac{1}{\mathbf{n}^2}\Big)\Big(\mathbf{N}\cdot\mathbf{F}^T_{\kappa_{p(t)}}\mathbf{D}\mathbf{F}_{\kappa_{p(t)}}\mathbf{N} - \mathbf{N}\cdot\mathbf{F}^T_{\kappa_{p(t)}}\mathbf{F}_{\kappa_{p(t)}}\mathbf{L}_{\kappa_{p(t)}}\mathbf{N}\Big). \tag{2.16}$$

We will for simplicity denote the factor $1-\frac{1}{|\mathbf{n}|^2}=\Gamma$. Following the same procedure as in the isotropic case, we arrive to the anisotropic dissipation in the form

$$\begin{aligned}\xi = \mathbf{T}\cdot\mathbf{D} - \mu\Big(\mathbf{B}_{\kappa_{p(t)}}\cdot\mathbf{D} - \mathbf{C}_{\kappa_{p(t)}}\cdot\mathbf{D}_{\kappa_{p(t)}} - \mathbf{I}\cdot\mathbf{D} + \mathbf{I}\cdot\mathbf{D}_{\kappa_{p(t)}}\Big)\\ - c\Gamma\Big(\mathbf{F}_{\kappa_{p(t)}}\mathbf{N}\otimes\mathbf{F}_{\kappa_{p(t)}}\mathbf{N}\Big)\cdot\mathbf{D} + c\Gamma\mathbf{F}^T_{\kappa_{p(t)}}\mathbf{F}_{\kappa_{p(t)}}\mathbf{N}\Big(\otimes\mathbf{N}\Big)\cdot\mathbf{L}_{\kappa_{p(t)}}.\end{aligned} \tag{2.17}$$

Rearanging the terms we arrive to

$$\begin{aligned}\xi = \Big[\mathbf{T}^d - \mu\mathbf{B}_{\kappa_{p(t)}} - c\Gamma\Big(\mathbf{N}\cdot\mathbf{F}^T_{\kappa_{p(t)}}\otimes\mathbf{F}_{\kappa_{p(t)}}\mathbf{N}\Big)\Big]\cdot\mathbf{D}\\ + \Big[\mu\Big(\mathbf{C}_{\kappa_{p(t)}}-\mathbf{I}\Big) + c\Gamma sym\Big(\mathbf{F}^T_{\kappa_{p(t)}}\mathbf{F}_{\kappa_{p(t)}}\mathbf{N}\otimes\mathbf{N}\Big)\Big]\cdot\mathbf{D}_{\kappa_{p(t)}}\\ + c\Gamma skew\Big(\mathbf{F}^T_{\kappa_{p(t)}}\mathbf{F}_{\kappa_{p(t)}}\mathbf{N}\otimes\mathbf{N}\Big)\cdot\mathbf{W}_{\kappa_{p(t)}}.\end{aligned} \tag{2.18}$$

Where we used the decomposition $\mathbf{L}_{\kappa_{p(t)}} = \mathbf{D}_{\kappa_{p(t)}} + \mathbf{W}_{\kappa_{p(t)}}$.

## 2.4 Closures

### 2.4.1 Anisotropic Giesekus model

We now similarly as in the Oldroyd-B model need to choose the appropriate relations that would create non-negative dissipation at all times. There is, yet again, a number of possible choices. We will first start with the simplest one being purely quadratic in all variables. The resulting relation is, however, nonlinear in $\mathbf{B}_{\kappa_{p(t)}}$. Later we will try to find a linear relation by finding the appropriate dissipation resulting in the linear constitutive model. Our first choice is

$$\xi = 2\nu\left|\mathbf{D}\right|^2 + 2\nu_1\left|\mathbf{D}_{\kappa_{p(t)}}\right|^2 + 2\nu_2\left|\mathbf{W}_{\kappa_{p(t)}}\right|^2,\ \nu,\nu_1,\nu_2>0. \tag{2.19}$$

One may notice that when $\nu_1=\nu_2$, we would be able to consider dissipation in terms of $\nu_1\mathbf{L}_{\kappa_{p(t)}}$ since

$$\begin{aligned}\left|\mathbf{L}_{\kappa_{p(t)}}\right|^2 = \left|\mathbf{D}_{\kappa_{p(t)}}+\mathbf{W}_{\kappa_{p(t)}}\right|^2 = \left|\mathbf{D}_{\kappa_{p(t)}}\right|^2 + \left|\mathbf{W}_{\kappa_{p(t)}}\right|^2 + \mathbf{D}_{\kappa_{p(t)}}\cdot\mathbf{W}_{\kappa_{p(t)}}\\ + \mathbf{W}_{\kappa_{p(t)}}\cdot\mathbf{D}_{\kappa_{p(t)}} = \left|\mathbf{D}_{\kappa_{p(t)}}\right|^2 + \left|\mathbf{W}_{\kappa_{p(t)}}\right|^2.\end{aligned} \tag{2.20}$$

Notice that $\mathbf{D}_{\kappa_{p(t)}}\cdot\mathbf{W}_{\kappa_{p(t)}} = \mathbf{W}_{\kappa_{p(t)}}\cdot\mathbf{D}_{\kappa_{p(t)}} = 0$ because we have a scalar product of a symmetric and a skew-symmetric tensor. From the prescribed dissipation we can now get the constitutive equations. From the first line of the dissipation we get

$$\mathbf{T}^d - \mu\mathbf{B}^d_{\kappa_{p(t)}} - c\Gamma\Big(\mathbf{F}_{\kappa_{p(t)}}\mathbf{N}\otimes\mathbf{F}_{\kappa_{p(t)}}\mathbf{N}\Big)^d = 2\nu\mathbf{D}^d. \tag{2.21}$$

Which yields after rearanging and using (2.2)

$$\mathbf{T}^d = 2\nu\mathbf{D}^d + \mu\mathbf{B}^d_{\kappa_{p(t)}} + c\Gamma\Big(\mathbf{n}\otimes\mathbf{n}\Big)^d. \tag{2.22}$$

Let us now examine the part $2\nu_1 \left|\mathbf{D}_{\kappa_{p(t)}}\right|^2$

$$\mu\Big(\mathbf{C}_{\kappa_{p(t)}} - \mathbf{I}\Big) + c\Gamma sym\Big(\mathbf{F}^T_{\kappa_{p(t)}}\mathbf{F}_{\kappa_{p(t)}}\mathbf{N}\otimes\mathbf{N}\Big) = 2\nu_1\mathbf{D}_{\kappa_{p(t)}}. \tag{2.23}$$

Substituting for $\mathbf{D}_{\kappa_{p(t)}}$ from (1.17) we get

$$\mu\Big(\mathbf{C}_{\kappa_{p(t)}} - \mathbf{I}\Big) + c\Gamma\Big(\mathbf{F}^T_{\kappa_{p(t)}}\mathbf{F}_{\kappa_{p(t)}}\mathbf{N}\otimes\mathbf{N}\Big) = -\nu_1\mathbf{F}^{-1}_{\kappa_{p(t)}}\overset{\triangledown}{\mathbf{B}}_{\kappa_{p(t)}}\mathbf{F}^{-T}_{\kappa_{p(t)}}. \tag{2.24}$$

We multiply the equation by $\mathbf{F}_{\kappa_{p(t)}}$ from the left and $\mathbf{F}^T_{\kappa_{p(t)}}$ from the right and get

$$\begin{aligned}\mu\mathbf{F}_{\kappa_{p(t)}}\Big(\mathbf{F}^T_{\kappa_{p(t)}}\mathbf{F}_{\kappa_{p(t)}} - \mathbf{I}\Big)\mathbf{F}^T_{\kappa_{p(t)}} + c\Gamma sym\Big(\mathbf{F}_{\kappa_{p(t)}}\mathbf{F}^T_{\kappa_{p(t)}}\mathbf{F}_{\kappa_{p(t)}}\mathbf{N}\otimes\mathbf{F}_{\kappa_{p(t)}}\mathbf{N}\Big)\\ +\nu_1\overset{\triangledown}{\mathbf{B}}_{\kappa_{p(t)}} = \mathbf{0},\end{aligned} \tag{2.25}$$

which after using (2.2) is

$$\mu\mathbf{B}_{\kappa_{p(t)}}\Big(\mathbf{B}_{\kappa_{p(t)}} - \mathbf{I}\Big) + c\Gamma sym\Big(\mathbf{B}_{\kappa_{p(t)}}\mathbf{n}\otimes\mathbf{n}\Big) + \nu_1\overset{\triangledown}{\mathbf{B}}_{\kappa_{p(t)}} = \mathbf{0}. \tag{2.26}$$

We will now address the dissipation $\nu_2\left|\mathbf{W}_{\kappa_{p(t)}}\right|^2$. We have

$$c\Gamma skew\Big(\mathbf{F}^T_{\kappa_{p(t)}}\mathbf{F}_{\kappa_{p(t)}}\mathbf{N}\otimes\mathbf{N}\Big) = 2\nu_2\mathbf{W}_{\kappa_{p(t)}}. \tag{2.27}$$

Now we multiply with $\mathbf{F}_{\kappa_{p(t)}}$ from the left and $\mathbf{F}^T_{\kappa_{p(t)}}$ from the right to be able to use the equation (1.25) and we end up with

$$\begin{aligned}c\Gamma skew\Big(\mathbf{B}_{\kappa_{p(t)}}\mathbf{n}\otimes\mathbf{n}\Big) &= 2\nu_2\mathbf{F}_{\kappa_{p(t)}}\mathbf{W}_{\kappa_{p(t)}}\mathbf{F}^T_{\kappa_{p(t)}}\\ &= 2\nu_2(-\mathbf{V}_{\kappa_{p(t)}}\mathbf{\Omega}_{\kappa_{p(t)}}\mathbf{V}_{\kappa_{p(t)}} + \mathbf{A}_{\mathbf{V}_{\kappa_{p(t)}}}).\end{aligned} \tag{2.28}$$

This gives us a complicated set of equations. Let us summarise

$$\begin{aligned}\operatorname{div}\mathbf{v} &= 0,\\ \rho\dot{\mathbf{v}} &= \operatorname{div}\mathbf{T},\\ \mathbf{T} &= -p\mathbf{I} + 2\nu\mathbf{D} + \mu\mathbf{B}^d_{\kappa_{p(t)}} + c\Gamma\Big(\mathbf{n}\otimes\mathbf{n}\Big)^d,\\ \mathbf{0} &= \mu\mathbf{B}_{\kappa_{p(t)}}\Big(\mathbf{B}_{\kappa_{p(t)}} - \mathbf{I}\Big) + c\Gamma sym\Big(\mathbf{B}_{\kappa_{p(t)}}\mathbf{n}\otimes\mathbf{n}\Big) + \nu_1\overset{\triangledown}{\mathbf{B}}_{\kappa_{p(t)}},\\ c\Gamma skew\Big(\mathbf{B}_{\kappa_{p(t)}}\mathbf{n}\otimes\mathbf{n}\Big) &= 2\nu_2(-\mathbf{V}_{\kappa_{p(t)}}\mathbf{\Omega}_{\kappa_{p(t)}}\mathbf{V}_{\kappa_{p(t)}} + \mathbf{A}_{\mathbf{V}_{\kappa_{p(t)}}}),\\ \dot{\mathbf{n}}^* &= \mathbf{\Omega}_{\kappa_{p(t)}}\mathbf{n}^*,\\ \mathbf{n} &= \mathbf{V}_{\kappa_{p(t)}}\mathbf{n}^*,\\ \mathbf{V}_{\kappa_{p(t)}}\mathbf{V}_{\kappa_{p(t)}} &= \mathbf{B}_{\kappa_{p(t)}}.\end{aligned}$$

We can further simplify the equations by realising

$$\dot{\mathbf{n}} = \dot{\overline{\mathbf{V}_{\kappa_{p(t)}}\mathbf{n}^*}} = \dot{\mathbf{V}}_{\kappa_{p(t)}}\mathbf{n}^* + \mathbf{V}_{\kappa_{p(t)}}\mathbf{\Omega}_{\kappa_{p(t)}}\mathbf{n}^*. \tag{2.29}$$

It will prove useful to multiply the equation (2.28) by a vector $\mathbf{V}^{-1}_{\kappa_{p(t)}}\mathbf{n}^*$. This leads to a vector equation

$$c\Gamma skew\Big(\mathbf{B}_{\kappa_{p(t)}}\mathbf{n}\otimes\mathbf{n}\Big)\mathbf{V}^{-1}_{\kappa_{p(t)}}\mathbf{n}^* = 2\nu_2(-\mathbf{V}_{\kappa_{p(t)}}\mathbf{\Omega}_{\kappa_{p(t)}}\mathbf{n}^* + \mathbf{A}_{\mathbf{V}_{\kappa_{p(t)}}}\mathbf{V}^{-1}_{\kappa_{p(t)}}\mathbf{n}^*), \quad (2.30)$$

where

$$\begin{aligned} &skew\Big(\mathbf{B}_{\kappa_{p(t)}}\mathbf{n}\otimes\mathbf{n}\Big)\mathbf{V}^{-1}_{\kappa_{p(t)}}\mathbf{n}^* \\ &\quad= \frac{1}{2}\Big(\mathbf{B}_{\kappa_{p(t)}}\mathbf{n}\otimes\mathbf{n}\Big)\mathbf{V}^{-1}_{\kappa_{p(t)}}\mathbf{n}^* - \frac{1}{2}\Big(\mathbf{n}\otimes\mathbf{B}_{\kappa_{p(t)}}\mathbf{n}\Big)\mathbf{V}^{-1}_{\kappa_{p(t)}}\mathbf{n}^* \\ &\quad= \frac{1}{2}\Big(\mathbf{B}_{\kappa_{p(t)}}\mathbf{n}\Big)\Big(\mathbf{n}^*\cdot\mathbf{V}_{\kappa_{p(t)}}\mathbf{V}^{-1}_{\kappa_{p(t)}}\mathbf{n}^*\Big) - \frac{1}{2}\mathbf{n}\Big(\mathbf{n}\cdot\mathbf{V}_{\kappa_{p(t)}}\mathbf{V}_{\kappa_{p(t)}}\mathbf{V}^{-1}_{\kappa_{p(t)}}\mathbf{n}^*\Big) \\ &\quad= \frac{1}{2}\Big(\mathbf{B}_{\kappa_{p(t)}}\mathbf{n}\Big)\Big(\mathbf{n}^*\cdot\mathbf{n}^*\Big) - \frac{1}{2}\mathbf{n}\Big(\mathbf{n}\cdot\mathbf{n}\Big) \\ &\quad= \frac{1}{2}\Big(\mathbf{B}_{\kappa_{p(t)}}\mathbf{n}\Big) - \frac{1}{2}\mathbf{n}\left|\mathbf{n}\right|^2, \end{aligned} \quad (2.31)$$

and

$$\begin{aligned} \mathbf{A}_{\mathbf{V}_{\kappa_{p(t)}}}\mathbf{V}^{-1}_{\kappa_{p(t)}}\mathbf{n}^* &= \frac{1}{2}\Big(\mathbf{V}_{\kappa_{p(t)}}\dot{\mathbf{V}}_{\kappa_{p(t)}}\mathbf{V}^{-1}_{\kappa_{p(t)}}\mathbf{n}^* - \dot{\mathbf{V}}_{\kappa_{p(t)}}\mathbf{n}^* + \mathbf{L}\mathbf{B}_{\kappa_{p(t)}}\mathbf{V}^{-1}_{\kappa_{p(t)}}\mathbf{n}^* \\ &\quad - \mathbf{B}_{\kappa_{p(t)}}\mathbf{L}^T\mathbf{V}^{-1}_{\kappa_{p(t)}}\mathbf{n}^*\Big) \\ &= \frac{1}{2}\Big(\mathbf{V}_{\kappa_{p(t)}}\dot{\mathbf{V}}_{\kappa_{p(t)}}\mathbf{V}^{-1}_{\kappa_{p(t)}}\mathbf{n}^* - \dot{\mathbf{V}}_{\kappa_{p(t)}}\mathbf{n}^* + \mathbf{L}\mathbf{n} \\ &\quad - \mathbf{B}_{\kappa_{p(t)}}\mathbf{L}^T\mathbf{V}^{-1}_{\kappa_{p(t)}}\mathbf{n}^*\Big). \end{aligned} \quad (2.32)$$

We further simplify (2.30) to the form

$$\begin{aligned} \frac{c\Gamma}{2}\Big(\mathbf{B}_{\kappa_{p(t)}}\mathbf{n} - \left|\mathbf{n}\right|^2\mathbf{n}\Big) + 2\nu_2\mathbf{V}_{\kappa_{p(t)}}\mathbf{\Omega}_{\kappa_{p(t)}}\mathbf{n}^* - \nu_2\mathbf{V}_{\kappa_{p(t)}}\dot{\mathbf{V}}_{\kappa_{p(t)}}\mathbf{V}^{-1}_{\kappa_{p(t)}}\mathbf{n}^* \\ +\nu_2\dot{\mathbf{V}}_{\kappa_{p(t)}}\mathbf{n}^* - \nu_2\mathbf{L}\mathbf{n} + \nu_2\mathbf{B}_{\kappa_{p(t)}}\mathbf{L}^T\mathbf{V}^{-1}_{\kappa_{p(t)}}\mathbf{n}^* = \mathbf{0}. \end{aligned} \quad (2.33)$$

The next step in order to obtain a simple model is to multiply the equation for $\mathbf{B}_{\kappa_{p(t)}}$ (2.26) with the same vector $\mathbf{V}^{-1}_{\kappa_{p(t)}}\mathbf{n}^*$. We then get

$$\begin{aligned} \mu\Big(\mathbf{B}_{\kappa_{p(t)}} - \mathbf{I}\Big)\mathbf{n} + \frac{c\Gamma}{2}\Big(\mathbf{B}_{\kappa_{p(t)}} + \left|\mathbf{n}\right|^2)\mathbf{n} + \nu_1\dot{\mathbf{V}}_{\kappa_{p(t)}}\mathbf{n}^* \\ +\nu_1\mathbf{V}_{\kappa_{p(t)}}\dot{\mathbf{V}}_{\kappa_{p(t)}}\mathbf{V}^{-1}_{\kappa_{p(t)}}\mathbf{n}^* - \nu_1\mathbf{L}\mathbf{n} - \nu_1\mathbf{B}_{\kappa_{p(t)}}\mathbf{L}^T\mathbf{V}^{-1}_{\kappa_{p(t)}}\mathbf{n}^* = \mathbf{n}. \end{aligned} \quad (2.34)$$

We now sum (2.33) $+\frac{\nu_2}{\nu_1}$ (2.34)

$$\begin{aligned} \mu\frac{\nu_2}{\nu_1}\Big(\mathbf{B}_{\kappa_{p(t)}} - \mathbf{I}\Big)\mathbf{n} + c\frac{\nu_2}{2\nu_1}\Gamma\Big(\mathbf{B}_{\kappa_{p(t)}} + \left|\mathbf{n}\right|^2\mathbf{I}\Big)\mathbf{n} + \frac{c\Gamma}{2}\Big(\mathbf{B}_{\kappa_{p(t)}} - \left|\mathbf{n}\right|^2\mathbf{I}\Big)\mathbf{n} \\ +2\nu_2\Big(\dot{\mathbf{V}}_{\kappa_{p(t)}}\mathbf{n}^* + \mathbf{V}_{\kappa_{p(t)}}\mathbf{\Omega}_{\kappa_{p(t)}}\mathbf{n}^* - \mathbf{L}\mathbf{n}\Big) = \mathbf{0}. \end{aligned} \quad (2.35)$$

Since we know that $\dot{\mathbf{V}}_{\kappa_{p(t)}}\mathbf{n}^* + \mathbf{V}_{\kappa_{p(t)}}\mathbf{\Omega}_{\kappa_{p(t)}}\mathbf{n}^* = \dot{\mathbf{n}}$ and we denote $\overset{\triangledown}{\mathbf{n}} = \dot{\mathbf{n}} - \mathbf{L}\mathbf{n}$, we can write

$$\begin{aligned} \mu\frac{\nu_2}{\nu_1}\Big(\mathbf{B}_{\kappa_{p(t)}} - \mathbf{I}\Big)\mathbf{n} + c\frac{\nu_2}{2\nu_1}\Gamma\Big(\mathbf{B}_{\kappa_{p(t)}} + \left|\mathbf{n}\right|^2\mathbf{I}\Big)\mathbf{n} + \frac{c\Gamma}{2}\Big(\mathbf{B}_{\kappa_{p(t)}} - \left|\mathbf{n}\right|^2\mathbf{I}\Big)\mathbf{n} \\ +2\nu_2\overset{\triangledown}{\mathbf{n}} = \mathbf{0}. \end{aligned} \quad (2.36)$$

In a more convenient form

$$\Big[\frac{(\nu_2+\nu_1)c\Gamma}{2\nu_1}+\mu\frac{\nu_2}{\nu_1}\Big]\mathbf{B}_{\kappa_{p(t)}}\mathbf{n}+\Big[\frac{(\nu_2-\nu_1)c\Gamma}{2\nu_1}\left|\mathbf{n}\right|^2-\mu\frac{\nu_2}{\nu_1}\Big]\mathbf{n}+2\nu_2\overset{\triangledown}{\mathbf{n}}=\mathbf{0}, \quad (2.37)$$

or even simpler

$$\Big((\nu_2+\nu_1)\mathbf{B}_{\kappa_{p(t)}}+(\nu_2-\nu_1)\left|\mathbf{n}\right|^2\mathbf{I}\Big)\frac{c\Gamma}{2\nu_1}\mathbf{n}+\mu\frac{\nu_2}{\nu_1}\Big(\mathbf{B}_{\kappa_{p(t)}}-\mathbf{I}\Big)\mathbf{n}+2\nu_2\overset{\triangledown}{\mathbf{n}}=\mathbf{0}. \quad (2.38)$$

This equation now lets us avoid direct calculation of several tensors and vectors namely $\mathbf{\Omega}_{\kappa_{p(t)}}, \mathbf{V}_{\kappa_{p(t)}}$ and $\mathbf{n}^*$. Out final summarised set of equations is therefore just

$$\begin{aligned}
\operatorname{div}\mathbf{v}&=0,\\
\rho\dot{\mathbf{v}}&=\operatorname{div}\mathbf{T},\\
\mathbf{T}&=-p\mathbf{I}+2\nu\mathbf{D}+\mu\mathbf{B}^d_{\kappa_{p(t)}}+c\Gamma\Big(\mathbf{n}\otimes\mathbf{n}\Big)^d,\\
\mathbf{0}&=\mu\mathbf{B}_{\kappa_{p(t)}}\Big(\mathbf{B}_{\kappa_{p(t)}}-\mathbf{I}\Big)+c\Gamma sym\Big(\mathbf{B}_{\kappa_{p(t)}}\mathbf{n}\otimes\mathbf{n}\Big)+\nu_1\overset{\triangledown}{\mathbf{B}}_{\kappa_{p(t)}},\\
\mathbf{0}&=\mu\frac{\nu_2}{\nu_1}\Big(\mathbf{B}_{\kappa_{p(t)}}-\mathbf{I}\Big)\mathbf{n}+\Big((\nu_2+\nu_1)\mathbf{B}_{\kappa_{p(t)}}+(\nu_2-\nu_1)\left|\mathbf{n}\right|^2\mathbf{I}\Big)\frac{c\Gamma}{2\nu_1}\mathbf{n}\\
&\quad+2\nu_2\overset{\triangledown}{\mathbf{n}}.
\end{aligned} \quad (2.39)$$

### 2.4.2 Anisotropic Oldroyd-B model

In order to get the linear relation we need to use the similar dissipation as with the isotropic Oldroyd-B model

$$\xi=2\nu\left|\mathbf{D}\right|^2+2\nu_1\mathbf{D}_{\kappa_{p(t)}}\mathbf{C}_{\kappa_{p(t)}}\cdot\mathbf{D}_{\kappa_{p(t)}}+2\nu_2\left|\mathbf{W}_{\kappa_{p(t)}}\right|^2. \quad (2.40)$$

This means the equation for the stress tensor (2.22) and equation for $\mathbf{\Omega}_{\kappa_{p(t)}}$ (2.28) will remain the same. The equation for $\mathbf{B}_{\kappa_{p(t)}}$ will, however, change. Before prescribing closures we will modify a bit the dissipation in $\mathbf{D}_{\kappa_{p(t)}}$. We split it into two processes and eventually show that they lead to a single linear equation

$$\begin{aligned}
\xi_{\mathbf{D}_{\kappa_{p(t)}}}&=\frac{1}{2}\Big[\mu\Big(\mathbf{C}_{\kappa_{p(t)}}-\mathbf{I}\Big)+c\Gamma\Big(\mathbf{F}^T_{\kappa_{p(t)}}\mathbf{F}_{\kappa_{p(t)}}\mathbf{N}\otimes\mathbf{N}\Big)\Big]\cdot\mathbf{D}_{\kappa_{p(t)}}\\
&\quad+\frac{1}{2}\Big[\mu\Big(\mathbf{C}_{\kappa_{p(t)}}-\mathbf{I}\Big)+c\Gamma\Big(\mathbf{N}\otimes\mathbf{F}^T_{\kappa_{p(t)}}\mathbf{F}_{\kappa_{p(t)}}\mathbf{N}\Big)\Big]\cdot\mathbf{D}_{\kappa_{p(t)}}.
\end{aligned} \quad (2.41)$$

First part of dissipation will be closed

$$\frac{1}{2}\Big[\mu\Big(\mathbf{C}_{\kappa_{p(t)}}-\mathbf{I}\Big)+c\Gamma\Big(\mathbf{F}^T_{\kappa_{p(t)}}\mathbf{F}_{\kappa_{p(t)}}\mathbf{N}\otimes\mathbf{N}\Big)\Big]=\nu_1\mathbf{C}_{\kappa_{p(t)}}\mathbf{D}_{\kappa_{p(t)}}. \quad (2.42)$$

We again as in the Oldroyd-B model multiply by $\mathbf{F}^{-T}_{\kappa_{p(t)}}$ from the left and $\mathbf{F}^T_{\kappa_{p(t)}}$ from the right and get

$$\frac{1}{2}\Big[\mu\Big(\mathbf{B}_{\kappa_{p(t)}}-\mathbf{I}\Big)+c\Gamma\Big(\mathbf{F}_{\kappa_{p(t)}}\mathbf{N}\otimes\mathbf{F}_{\kappa_{p(t)}}\mathbf{N}\Big)\Big]=\nu_1\mathbf{F}_{\kappa_{p(t)}}\mathbf{D}_{\kappa_{p(t)}}\mathbf{F}^T_{\kappa_{p(t)}}. \quad (2.43)$$

Using (1.17) and (2.2)

$$\mu\Big(\mathbf{B}_{\kappa_{p(t)}}-\mathbf{I}\Big)+c\Gamma\Big(\mathbf{n}\otimes\mathbf{n}\Big)+\nu_1\overset{\triangledown}{\mathbf{B}}_{\kappa_{p(t)}}=\mathbf{0}. \quad (2.44)$$

Second part of $\xi_{\mathbf{D}_{\kappa_{p(t)}}}$ is addressed in a similar way

$$\frac{1}{2}\Big[\mu\Big(\mathbf{C}_{\kappa_{p(t)}}-\mathbf{I}\Big)+c\Gamma\Big(\mathbf{N}\otimes\mathbf{F}^T_{\kappa_{p(t)}}\mathbf{F}_{\kappa_{p(t)}}\mathbf{N}\Big)\Big]=\nu_1\mathbf{D}_{\kappa_{p(t)}}\mathbf{C}_{\kappa_{p(t)}}, \tag{2.45}$$

except we multiply with $\mathbf{F}_{\kappa_{p(t)}}$ from the left and $\mathbf{F}^{-1}_{\kappa_{p(t)}}$ from the right

$$\frac{1}{2}\Big[\mu\Big(\mathbf{B}_{\kappa_{p(t)}}-\mathbf{I}\Big)+c\Gamma\Big(\mathbf{F}_{\kappa_{p(t)}}\mathbf{N}\otimes\mathbf{F}_{\kappa_{p(t)}}\mathbf{N}\Big)\Big]=\nu_1\mathbf{F}_{\kappa_{p(t)}}\mathbf{D}_{\kappa_{p(t)}}\mathbf{F}^T_{\kappa_{p(t)}}, \tag{2.46}$$

Again using (1.17) and (2.2) gives us

$$\mu\Big(\mathbf{B}_{\kappa_{p(t)}}-\mathbf{I}\Big)+c\Gamma\Big(\mathbf{n}\otimes\mathbf{n}\Big)+\nu_1\overset{\triangledown}{\mathbf{B}}_{\kappa_{p(t)}}=\mathbf{0}, \tag{2.47}$$

Which is exactly equation (2.44). This means we only have one consistent equation for $\mathbf{B}_{\kappa_{p(t)}}$, even though we started with the splitting of dissipation. Sumarising the equations for this particular linear model we have

$$\begin{aligned}
\operatorname{div}\mathbf{v}&=0,\\
\rho\dot{\mathbf{v}}&=\operatorname{div}\mathbf{T},\\
\mathbf{T}&=-p\mathbf{I}+2\nu\mathbf{D}+\mu\mathbf{B}^d_{\kappa_{p(t)}}+c\Gamma\Big(\mathbf{n}\otimes\mathbf{n}\Big)^d,\\
\mathbf{0}&=\mu\Big(\mathbf{B}_{\kappa_{p(t)}}-\mathbf{I}\Big)+c\Gamma\Big(\mathbf{n}\otimes\mathbf{n}\Big)+\nu_1\overset{\triangledown}{\mathbf{B}}_{\kappa_{p(t)}},\\
c\Gamma skew\Big(\mathbf{B}_{\kappa_{p(t)}}\mathbf{n}\otimes\mathbf{n}\Big)&=2\nu_2(-\mathbf{V}_{\kappa_{p(t)}}\mathbf{\Omega}_{\kappa_{p(t)}}\mathbf{V}_{\kappa_{p(t)}}+\mathbf{A}_{\mathbf{V}_{\kappa_{p(t)}}}),\\
\dot{\mathbf{n}^*}&=\mathbf{\Omega}_{\kappa_{p(t)}}\mathbf{n}^*,\\
\mathbf{n}&=\mathbf{V}_{\kappa_{p(t)}}\mathbf{n}^*,\\
\mathbf{V}_{\kappa_{p(t)}}\mathbf{V}_{\kappa_{p(t)}}&=\mathbf{B}_{\kappa_{p(t)}}.
\end{aligned}$$

This model can be simplified in the same way as the anisotropic model with quadratic dissipation. We first multiply (2.28) with $\mathbf{V}^{-1}_{\kappa_{p(t)}}\mathbf{n}^*$. and get (2.33). We, however, have a different equation for $\mathbf{B}_{\kappa_{p(t)}}$ which we multiply with $\mathbf{V}^{-1}_{\kappa_{p(t)}}\mathbf{n}^*$ and get

$$\begin{aligned}
\mu\Big(\mathbf{n}-\mathbf{V}^{-1}_{\kappa_{p(t)}}\mathbf{n}^*\Big)+c\Gamma\mathbf{n}+\nu_1\dot{\mathbf{V}}_{\kappa_{p(t)}}\mathbf{n}^*+\nu_1\mathbf{V}_{\kappa_{p(t)}}\dot{\mathbf{V}}_{\kappa_{p(t)}}\mathbf{V}^{-1}_{\kappa_{p(t)}}\mathbf{n}^*\\
-\nu_1\mathbf{L}\mathbf{n}-\nu_1\mathbf{B}_{\kappa_{p(t)}}\mathbf{L}^T\mathbf{V}^{-1}_{\kappa_{p(t)}}\mathbf{n}^*=\mathbf{0}.
\end{aligned} \tag{2.48}$$

We now sum the equation (2.33) + $\frac{\nu_2}{\nu_1}$ (2.48) and obtain

$$\mu\frac{\nu_2}{\nu_1}\Big(\mathbf{n}-\mathbf{V}^{-1}_{\kappa_{p(t)}}\mathbf{n}^*\Big)+c\frac{\nu_2}{\nu_1}\Gamma\mathbf{n}+\frac{c\Gamma}{2}\Big(\mathbf{B}_{\kappa_{p(t)}}-|\mathbf{n}|^2\,\mathbf{I}\Big)\mathbf{n}+2\nu_2\overset{\triangledown}{\mathbf{n}}=\mathbf{0}. \tag{2.49}$$

Moreover, in order to create a model in terms of $\mathbf{B}_{\kappa_{p(t)}}$ and $\mathbf{n}$ without a need to calculate any inverse tensors, we multiply the equation with tensor $\mathbf{B}_{\kappa_{p(t)}}$ from the left

$$\begin{aligned}
\mu\frac{\nu_2}{\nu_1}\Big(\mathbf{B}_{\kappa_{p(t)}}-\mathbf{I}\Big)\mathbf{n}+c\frac{\nu_2}{\nu_1}\Gamma\mathbf{B}_{\kappa_{p(t)}}\mathbf{n}+\frac{c\Gamma}{2}\Big(\mathbf{B}_{\kappa_{p(t)}}-|\mathbf{n}|^2\Big)\mathbf{B}_{\kappa_{p(t)}}\mathbf{n}\\
+2\nu_2\mathbf{B}_{\kappa_{p(t)}}\overset{\triangledown}{\mathbf{n}}=\mathbf{0}.
\end{aligned} \tag{2.50}$$

Final set of equation is

$$\begin{aligned}
\operatorname{div}\mathbf{v} &= 0,\\
\rho\dot{\mathbf{v}} &= \operatorname{div}\mathbf{T},\\
\mathbf{T} &= -p\mathbf{I} + 2\nu\mathbf{D} + \mu\mathbf{B}^d_{\kappa_{p(t)}} + c\Gamma\Big(\mathbf{n}\otimes\mathbf{n}\Big)^d,\\
\mathbf{0} &= \mu\Big(\mathbf{B}_{\kappa_{p(t)}} - \mathbf{I}\Big) + c\Gamma\Big(\mathbf{n}\otimes\mathbf{n}\Big) + \nu_1\overset{\triangledown}{\mathbf{B}}_{\kappa_{p(t)}},\\
\mathbf{0} &= \mu\frac{\nu_2}{\nu_1}\Big(\mathbf{B}_{\kappa_{p(t)}} - \mathbf{I}\Big)\mathbf{n} + c\frac{\nu_2}{\nu_1}\Gamma\mathbf{B}_{\kappa_{p(t)}}\mathbf{n}\\
&\quad + \frac{c\Gamma}{2}\Big(\mathbf{B}_{\kappa_{p(t)}} - |\mathbf{n}|^2\Big)\mathbf{B}_{\kappa_{p(t)}}\mathbf{n} + 2\nu_2\mathbf{B}_{\kappa_{p(t)}}\overset{\triangledown}{\mathbf{n}}.
\end{aligned} \tag{2.51}$$

We will further refer to this model as to the anisotropic Oldroyd-B model.

### 2.4.3 Model non-dissipative in $\mathbf{W}_{\kappa_{p(t)}}$

In general, parameters $\nu, \nu_1, \nu_2$ are independent. An interesting and rather simple model is obtained when considering dissipation

$$\xi = 2\nu\mathbf{D}^2 + 2\nu_1\mathbf{D}_{\kappa_{p(t)}}\mathbf{C}_{\kappa_{p(t)}}\cdot\mathbf{D}_{\kappa_{p(t)}} + 2\nu_2\left|\mathbf{W}_{\kappa_{p(t)}}\right|^2, \tag{2.52}$$

while setting $\nu_2 = 0$. This leaves us with dissipation only in the symmetric part of $\mathbf{L}_{\kappa_{p(t)}}$. The only equation we need to modify from the previous model is the equation (2.27) which reduces to

$$c\Gamma skew\Big(\mathbf{C}_{\kappa_{p(t)}}\mathbf{N}\otimes\mathbf{N}\Big) = \mathbf{0}. \tag{2.53}$$

Since $c$ and $\Gamma$ are in our case possitive, we are solving for

$$\Big(\mathbf{C}_{\kappa_{p(t)}}\mathbf{N}\otimes\mathbf{N}\Big) - \Big(\mathbf{N}\otimes\mathbf{C}_{\kappa_{p(t)}}\mathbf{N}\Big) = \mathbf{0}. \tag{2.54}$$

We multiply with $\mathbf{R}_{\kappa_{p(t)}}$ from the left and $\mathbf{R}^T_{\kappa_{p(t)}}$ from the right and get

$$\Big(\mathbf{B}_{\kappa_{p(t)}}\mathbf{n}^*\otimes\mathbf{n}^*\Big) - \Big(\mathbf{n}^*\otimes\mathbf{B}_{\kappa_{p(t)}}\mathbf{n}^*\Big) = \mathbf{0}. \tag{2.55}$$

This can be further simplified when written in coordinates as

$$(\mathbf{B}_{\kappa_{p(t)}})_{ij}\mathbf{n}^*_j\mathbf{n}^*_k - \mathbf{n}^*_i(\mathbf{B}_{\kappa_{p(t)}})_{kj}\mathbf{n}^*_j = \mathbf{0}. \tag{2.56}$$

We can best see the meaning of this expression when we consider vector representation of the obtained skew-symmetric matrix

$$\begin{pmatrix} 0 & a & -b\\ -a & 0 & c\\ b & -c & 0\end{pmatrix} \Rightarrow \begin{pmatrix} c\\ b\\ a\end{pmatrix}. \tag{2.57}$$

This leaves us with

$$\begin{pmatrix}(\mathbf{B}_{\kappa_{p(t)}})_{2j}\mathbf{n}^*_j\mathbf{n}^*_3 - (\mathbf{B}_{\kappa_{p(t)}})_{3j}\mathbf{n}^*_j\mathbf{n}^*_2\\ (\mathbf{B}_{\kappa_{p(t)}})_{3j}\mathbf{n}^*_j\mathbf{n}^*_1 - (\mathbf{B}_{\kappa_{p(t)}})_{1j}\mathbf{n}^*_j\mathbf{n}^*_3\\ (\mathbf{B}_{\kappa_{p(t)}})_{1j}\mathbf{n}^*_j\mathbf{n}^*_2 - (\mathbf{B}_{\kappa_{p(t)}})_{2j}\mathbf{n}^*_j\mathbf{n}^*_1\end{pmatrix} = \mathbf{0}. \tag{2.58}$$

Vector on the left side of the equation is in three dimensions known as a vector product of vectors $\mathbf{B}_{\kappa_{p(t)}}\mathbf{n}^*$ and $\mathbf{n}^*$. Since

$$\mathbf{B}_{\kappa_{p(t)}}\mathbf{n}^* \times \mathbf{n}^* = \mathbf{0}, \tag{2.59}$$

vectors $\mathbf{B}_{\kappa_{p(t)}}\mathbf{n}^*$ and $\mathbf{n}^*$ are colinear. In other words

$$\mathbf{B}_{\kappa_{p(t)}}\mathbf{n}^* = \lambda\mathbf{n}^*, \tag{2.60}$$

This means that $\mathbf{n}^*$ is an eigenvector of $\mathbf{B}_{\kappa_{p(t)}}$ with an eigenvalue $\lambda$. The final set of equations that we use is

$$\begin{aligned}
\operatorname{div}\mathbf{v} &= 0,\\
\rho\dot{\mathbf{v}} &= \operatorname{div}\mathbf{T},\\
\mathbf{T} &= -p\mathbf{I} + 2\nu\mathbf{D} + \mu\mathbf{B}^d_{\kappa_{p(t)}} + c\Gamma\Big(\mathbf{n}\otimes\mathbf{n}\Big)^d,\\
\mathbf{0} &= \mu\Big(\mathbf{B}_{\kappa_{p(t)}} - \mathbf{I}\Big) + c\Gamma\Big(\mathbf{n}\otimes\mathbf{n}\Big) + \nu_1\overset{\triangledown}{\mathbf{B}}_{\kappa_{p(t)}},\\
\mathbf{B}_{\kappa_{p(t)}}\mathbf{n}^* \times \mathbf{n}^* &= \mathbf{0},\\
\mathbf{n} &= \mathbf{V}_{\kappa_{p(t)}}\mathbf{n}^*,\\
\mathbf{V}_{\kappa_{p(t)}}\mathbf{V}_{\kappa_{p(t)}} &= \mathbf{B}_{\kappa_{p(t)}},\\
\mathbf{n}^*\cdot\mathbf{n}^* &= 1.
\end{aligned} \tag{2.61}$$

These equations can be in some cases simplified. One such simplification will be given in the numerical part of this thesis.

### 2.4.4 Model with $\nu_1 = \nu_2$

Another special case that can be investigated is the equal viscosities case $\nu_1 = \nu_2$. This will simplify the equations. We are able to proceed by using two different approaches. One is to calculate the limit $\nu_2 \to \nu_1$ in (2.38). We however, choose to obtain the equations by merging the dissipation in $\mathbf{W}_{\kappa_{p(t)}}$ with $\mathbf{D}_{\kappa_{p(t)}}$ and simply write the resulting dissipation as

$$\begin{aligned}
\xi = &\left[\mathbf{T}^d - \mu\mathbf{B}_{\kappa_{p(t)}} - c\Gamma\Big(\mathbf{N}\cdot\mathbf{F}^T_{\kappa_{p(t)}}\otimes\mathbf{F}_{\kappa_{p(t)}}\mathbf{N}\Big)\right]\cdot\mathbf{D}\\
&+\left[\mu\Big(\mathbf{C}_{\kappa_{p(t)}} - \mathbf{I}\Big) + c\Gamma\Big(\mathbf{F}^T_{\kappa_{p(t)}}\mathbf{F}_{\kappa_{p(t)}}\mathbf{N}\otimes\mathbf{N}\Big)\right]\cdot\mathbf{L}_{\kappa_{p(t)}}.
\end{aligned} \tag{2.62}$$

We prescribe the simplest quadratic dissipation

$$\xi = 2\nu\left|\mathbf{D}\right|^2 + 2\nu_1\left|\mathbf{L}_{\kappa_{p(t)}}\right|^2. \tag{2.63}$$

That yields an unchanged equation for the Cauchy stress tensor (2.22) and an equation for $\mathbf{F}_{\kappa_{p(t)}}$

$$\mu\Big(\mathbf{C}_{\kappa_{p(t)}} - \mathbf{I}\Big) + c\Gamma\Big(\mathbf{F}^T_{\kappa_{p(t)}}\mathbf{F}_{\kappa_{p(t)}}\mathbf{N}\otimes\mathbf{N}\Big) = 2\nu_1\mathbf{L}_{\kappa_{p(t)}}. \tag{2.64}$$

We will now use the equation (1.14) that gives us the formula for $\mathbf{L}_{\kappa_{p(t)}}$

$$\mathbf{L}_{\kappa_{p(t)}} = \mathbf{F}^{-1}_{\kappa_{p(t)}}\Big(\mathbf{L}\mathbf{F}_{\kappa_{p(t)}} - \dot{\mathbf{F}}_{\kappa_{p(t)}}\Big) = -\mathbf{F}^{-1}_{\kappa_{p(t)}}\Big(\dot{\mathbf{F}}_{\kappa_{p(t)}} - \mathbf{L}\mathbf{F}_{\kappa_{p(t)}}\Big), \tag{2.65}$$

The last two equations give together

$$\begin{aligned}\mu\Big(\mathbf{C}_{\kappa_{p(t)}}-\mathbf{I}\Big)+c\Gamma\Big(\mathbf{F}^T_{\kappa_{p(t)}}\mathbf{F}_{\kappa_{p(t)}}\mathbf{N}\otimes\mathbf{N}\Big)\\ =-2\nu_1\mathbf{F}^{-1}_{\kappa_{p(t)}}\Big(\dot{\mathbf{F}}_{\kappa_{p(t)}}-\mathbf{L}\mathbf{F}_{\kappa_{p(t)}}\Big).\end{aligned}\tag{2.66}$$

We will now try to simplify the equations by multiplying with $\mathbf{F}_{\kappa_{p(t)}}$ from the left

$$\begin{aligned}\mu\mathbf{F}_{\kappa_{p(t)}}\Big(\mathbf{F}^T_{\kappa_{p(t)}}\mathbf{F}_{\kappa_{p(t)}}-\mathbf{I}\Big)+c\Gamma\Big(\mathbf{F}_{\kappa_{p(t)}}\mathbf{F}^T_{\kappa_{p(t)}}\mathbf{F}_{\kappa_{p(t)}}\mathbf{N}\otimes\mathbf{N}\Big)\\ +2\nu_1\Big(\dot{\mathbf{F}}_{\kappa_{p(t)}}-\mathbf{L}\mathbf{F}_{\kappa_{p(t)}}\Big)=\mathbf{0}.\end{aligned}\tag{2.67}$$

We are able to use this equations for practical calculation considering $\mathbf{F}_{\kappa_{p(t)}}$ as a variable. However we choose to rewrite the equation in a more familiar manner - in terms of $\mathbf{B}_{\kappa_{p(t)}}$ and $\mathbf{n}$. For this we will first need to transpose equation (2.67)

$$\begin{aligned}\mu\mathbf{F}^T_{\kappa_{p(t)}}\Big(\mathbf{F}_{\kappa_{p(t)}}\mathbf{F}^T_{\kappa_{p(t)}}-\mathbf{I}\Big)+c\Gamma\Big(\mathbf{N}\otimes\mathbf{F}_{\kappa_{p(t)}}\mathbf{F}^T_{\kappa_{p(t)}}\mathbf{F}_{\kappa_{p(t)}}\mathbf{N}\Big)\\ +2\nu_1\Big(\dot{\mathbf{F}}^T_{\kappa_{p(t)}}-\mathbf{F}^T_{\kappa_{p(t)}}\mathbf{L}^T\Big)=\mathbf{0}.\end{aligned}\tag{2.68}$$

We will now multiply the original equation with $\mathbf{F}^T_{\kappa_{p(t)}}$ from the right and the transposed equation with $\mathbf{F}_{\kappa_{p(t)}}$ from the left. Using $\mathbf{F}_{\kappa_{p(t)}}\mathbf{F}^T_{\kappa_{p(t)}}=\mathbf{B}_{\kappa_{p(t)}}$ and (2.2) we get

$$\begin{aligned}\mu\mathbf{B}_{\kappa_{p(t)}}\Big(\mathbf{B}_{\kappa_{p(t)}}-\mathbf{I}\Big)+c\Gamma\Big(\mathbf{B}_{\kappa_{p(t)}}\mathbf{n}\otimes\mathbf{n}\Big)\\ +2\nu_1\Big(\dot{\mathbf{F}}_{\kappa_{p(t)}}\mathbf{F}^T_{\kappa_{p(t)}}-\mathbf{L}\mathbf{B}_{\kappa_{p(t)}}\Big)=\mathbf{0},\end{aligned}\tag{2.69}$$

$$\begin{aligned}\mu\mathbf{B}_{\kappa_{p(t)}}\Big(\mathbf{B}_{\kappa_{p(t)}}-\mathbf{I}\Big)+c\Gamma\Big(\mathbf{n}\otimes\mathbf{B}_{\kappa_{p(t)}}\mathbf{n}\Big)\\ +2\nu_1\Big(\mathbf{F}_{\kappa_{p(t)}}\dot{\mathbf{F}}^T_{\kappa_{p(t)}}-\mathbf{B}_{\kappa_{p(t)}}\mathbf{L}^T\Big)=\mathbf{0}.\end{aligned}\tag{2.70}$$

Now, we sum both equations (taking only a half of each one) and using $\dot{\mathbf{B}}_{\kappa_{p(t)}}=\dot{\mathbf{F}}_{\kappa_{p(t)}}\mathbf{F}^T_{\kappa_{p(t)}}+\mathbf{F}_{\kappa_{p(t)}}\dot{\mathbf{F}}^T_{\kappa_{p(t)}}$ get

$$\begin{aligned}\mu\mathbf{B}_{\kappa_{p(t)}}\Big(\mathbf{B}_{\kappa_{p(t)}}-\mathbf{I}\Big)+\frac{c}{2}\Gamma\Big[\Big(\mathbf{n}\otimes\mathbf{B}_{\kappa_{p(t)}}\mathbf{n}\Big)+\Big(\mathbf{B}_{\kappa_{p(t)}}\mathbf{n}\otimes\mathbf{n}\Big)\Big]\\ +\nu_1\Big(\dot{\mathbf{B}}_{\kappa_{p(t)}}-\mathbf{L}\mathbf{B}_{\kappa_{p(t)}}-\mathbf{B}_{\kappa_{p(t)}}\mathbf{L}^T\Big)=\mathbf{0},\end{aligned}\tag{2.71}$$

where we can identify the objective derivative of $\overset{\triangledown}{\mathbf{B}}_{\kappa_{p(t)}}=\dot{\mathbf{B}}_{\kappa_{p(t)}}-\mathbf{L}\mathbf{B}_{\kappa_{p(t)}}-\mathbf{B}_{\kappa_{p(t)}}\mathbf{L}^T$

$$\mu\mathbf{B}_{\kappa_{p(t)}}\Big(\mathbf{B}_{\kappa_{p(t)}}-\mathbf{I}\Big)+c\Gamma sym\Big(\mathbf{n}\otimes\mathbf{B}_{\kappa_{p(t)}}\mathbf{n}\Big)+\nu_1\overset{\triangledown}{\mathbf{B}}_{\kappa_{p(t)}}=\mathbf{0}.\tag{2.72}$$

There is another equation we need to identify. Equation for $\mathbf{n}$. To obtain this equation we simply multiply (2.67) by $\mathbf{N}$ from the right

$$\begin{aligned}\mu\mathbf{F}_{\kappa_{p(t)}}\Big(\mathbf{F}^T_{\kappa_{p(t)}}\mathbf{F}_{\kappa_{p(t)}}\mathbf{N}-\mathbf{N}\Big)+c\Gamma\Big(\mathbf{F}_{\kappa_{p(t)}}\mathbf{F}^T_{\kappa_{p(t)}}\mathbf{F}_{\kappa_{p(t)}}\mathbf{N}\otimes\mathbf{N}\Big)\mathbf{N}\\ +2\nu_1\Big(\dot{\mathbf{F}}_{\kappa_{p(t)}}\mathbf{N}-\mathbf{L}\mathbf{F}_{\kappa_{p(t)}}\mathbf{N}\Big)=\mathbf{0}.\end{aligned}\tag{2.73}$$

Now simply using (2.2)

$$\mu\Big(\mathbf{B}_{\kappa_{p(t)}}-\mathbf{I}\Big)\mathbf{n}+c\Gamma\mathbf{B}_{\kappa_{p(t)}}\mathbf{n}+2\nu_1\Big(\dot{\mathbf{n}}-\mathbf{L}\mathbf{n}\Big)=\mathbf{0}.\tag{2.74}$$

Recognising objective derivative for vector quantity we simplify the equation to

$$\mu\Big(\mathbf{B}_{\kappa_{p(t)}} - \mathbf{I}\Big)\mathbf{n} + c\Gamma\mathbf{B}_{\kappa_{p(t)}}\mathbf{n} + 2\nu_1\overset{\triangledown}{\mathbf{n}} = \mathbf{0}. \tag{2.75}$$

To summarise the equations

$$\begin{aligned}
\operatorname{div}\mathbf{v} &= 0,\\
\rho\dot{\mathbf{v}} &= \operatorname{div}\mathbf{T},\\
\mathbf{T} &= -p\mathbf{I} + 2\nu\mathbf{D} + \mu\mathbf{B}^d_{\kappa_{p(t)}} + c\Gamma\Big(\mathbf{n}\otimes\mathbf{n}\Big)^d,\\
\mathbf{0} &= \mu\mathbf{B}_{\kappa_{p(t)}}\Big(\mathbf{B}_{\kappa_{p(t)}} - \mathbf{I}\Big) + c\Gamma sym\Big(\mathbf{B}_{\kappa_{p(t)}}\mathbf{n}\otimes\mathbf{n}\Big) + \nu_1\overset{\triangledown}{\mathbf{B}}_{\kappa_{p(t)}},\\
\mathbf{0} &= \mu\Big(\mathbf{B}_{\kappa_{p(t)}} - \mathbf{I}\Big)\mathbf{n} + c\Gamma\mathbf{B}_{\kappa_{p(t)}}\mathbf{n} + 2\nu_1\overset{\triangledown}{\mathbf{n}}.
\end{aligned} \tag{2.76}$$

We will now show that we are able to obtain the same result by a limit transition $\nu_2 \to \nu_1$ in the equations of a model (2.39). The equations are the same as we just derived, except for the last one (2.38), the evolution equation for $\mathbf{n}$. When we perform the limit we get

$$\mu\frac{\nu_1}{\nu_1}\Big(\mathbf{B}_{\kappa_{p(t)}} - \mathbf{I}\Big)\mathbf{n} + \Big((\nu_1+\nu_1)\mathbf{B}_{\kappa_{p(t)}} + (\nu_1-\nu_1)\left|\mathbf{n}\right|^2\Big)\frac{c\Gamma}{2\nu_1}\mathbf{n} + 2\nu_1\overset{\triangledown}{\mathbf{n}} = \mathbf{0}. \tag{2.77}$$

After we simplify

$$\mu\Big(\mathbf{B}_{\kappa_{p(t)}} - \mathbf{I}\Big)\mathbf{n} + c\Gamma\mathbf{B}_{\kappa_{p(t)}}\mathbf{n} + 2\nu_1\overset{\triangledown}{\mathbf{n}} = \mathbf{0}, \tag{2.78}$$

which is the same result as we derived in this section using the dissipation in $\mathbf{L}_{\kappa_{p(t)}}$.

# 3. Motivation

## 3.1 Liquid crystals

One of the natural ways to understand the models developed in the previous chapters is to think about them as a form of a fluid with rod-like structures. In practice such materials are present in a form of various classes of liquid crystals that can exist in numerous phases. One way to categorise them is depending on what influences their phase transition behaviour.

- Thermotropic liquid crystals that change phase depending on the temperature.
- Lyotropic liquid crystals phase transition is influenced by temperature but also by the concentration of the crystals in the solvent.
- Metallotropic liquid crystals are composed of mixture of organic and anorganic components and in addition to temperature and concentration in solvent, the ratio between organic and anorganic composition also influences the phase of a liquid crystal.

Various liquid crystal phases occur in nature. They are frequently present in biological tissues or in many technical applications. Most current electronic displays use their ability to influence the orientation of the crystal structures to shade the passing polarised light. The understanding and modeling of liquid crystals is therefore of great interest for sciencists for over fifty years now. Various constitutive models have been developed describing particular phase and certain phenomena occuring in liquid crystals. Among the most famous are the models of Oseen-Frank [11], models of Leslie [12] or so called Landau–de Gennes model [13]. We, in the scope of this thesis have no ambition of improving this models. However, since our models are derived from very minimal assumptions, we seek to find qualitative proofs that the behaviour of our models is similar to the real world liquid crystals.

### 3.1.1 Tumbling phenomenon

One of the well known phenomenon concerning liquid crystal shear flow is whether the crystals tumble or align with the flow. The Leslie-Ericksen $\mathbf{n}$-vector theory predicts the behaviour and introduces a parameter $\lambda$, called tumbling parameter. When this parameter is above 1, the crystals tends to align with the flow. However, when $\lambda < 1$ $\mathbf{n}$-vector tends to tumble. Various methods to measure and analyse tumbling behaviour can be found in [14]. The paper proposes different ways how to measure the orientation of anisotropy in liquid crystals. One such method, measuring the shear stress resulting from Couette flow will be investigated and calculated in the following sections. We will calculate the apparent viscosity defined as

$$\eta = \frac{\tau}{\dot{\gamma}}, \tag{3.1}$$

where $\tau$ represents the shear stress and $\dot{\gamma}$ is the shear rate. In our simulations the shear stress can be calculated and is well defined. Calculation of a shear rate is not straight-forward for general geometries. However, it has a clear meaning in the case of so called simple Couette flow.

### 3.1.2 Simple Couette flow

Geometry of the Couette flow can be seen in the Figure 4.1, $v_{top}$ is the velocity of a moving upper plate that causes the flow, $h$ is the distance between the top and the bottom plate. In the case of Newtonian fluid, this problem has an analytical solution. The velocity has a linear profile being zero on the lower plate and $v_{top}$ on the upper plate. The same can be analyticaly calculated for the Oldroyd-B fluid and for the Giesekus model. Moreover since the solutions are linear in velocity and constant in other variable, the solution is exact using finite elements linear in pressure and quadratic in other variables. In all mentioned cases, all variables describing the flow are constant in $x$ direction. We will see that the same applies for anisotropic models developed in this thesis. Using this knowledge the folowing relation can be used to calculate the shear rate

$$\dot{\gamma} = \frac{v_{top}}{h}. \tag{3.2}$$

This experiment is a 2D experiment and will serve as a useful toy problem to get an insight on how the developed anisotropic models behave. We will investigate general behaviour in shear and plot the evolution of the apparent viscosity. We will try to decide whether the vector $\mathbf{n}$ from our developed models tumbles or aligns with the flow. More generally we will try to decide if a model evolves into a steady state.

### 3.1.3 Rheological experiment

More realistic problem we will be solving is a 3D evolution. We try to simulate the problem described in the aforementioned paper [14]. The authors used a cone-and-plate geometry Rheometrics ARES rheometer. This rheometer consists of a fixed plate at the bottom and a cone with very small angle of 0.04 radians at the top. The cone rotates and creates a shear flow. The vector of anisotropy field is initially uniform. Rotation is then started and an apparent viscosity is measured. We can see the geometry in the Figure 3.1. The reason this rheometer is made

Figure 3.1: Cone and plate rheometer

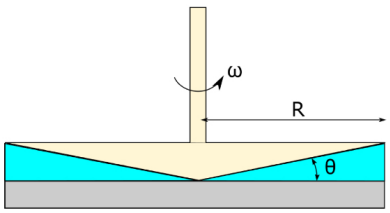


using this geometry is that we can evaluate the shear rate that is theoreticaly constant in the domain. We consider the shear rate relation 3.2. The cone velocity

scales with the distance from the center $r$ as $\mathbf{v} = \omega \cdot r$, where $\omega$ is the angular velocity of the rotating cone. The height of shearing fluid scales as $h = \theta \cdot r$, where since $\theta$ is small we used an approximation $\tan(\theta) \approx \theta$. The shear rate for this geometry is therefore

$$\dot{\gamma} = \frac{\omega \cdot r}{\theta \cdot r} = \frac{\omega}{\theta}. \tag{3.3}$$

We can see it is independent on the distance from the center therefore it is constant for the rheometer.

### 3.1.4 3D simulation

We will try to simulate the experiment. However, the geometry of the cone and plate rheometer has its complications. The ratio between the height and width of the computational domain is only 0.04. This poses a problem since we would like to maintain the reasonable vertical resolution, wich requires a large amount of elements if we want them not to be completely flatened. Next, there is discontinuity present in the domain. Shear rate in the point on the tip of the cone is 0 while it is non-zero and constant everywhere else. Therefore, since the numerical properties of the model have not been yet studied, we have chosen a simplified version of the problem. We will consider just two parallel plates, the top one moving with angular velocity $\omega$ and the bottom one still. This geometry is easier to mesh and calculate with, however it has a flaw. The shear rate is not constant. We therefore calculate just shear stress integrated over the top plate divided by the integrated shear rate denoting it $\overline{\eta}$. This is not the apparent viscosity as defined above nontheless it serves to give an insight on how the model behaves in the 3D geometry similar to the experimental one.

# 4. Simulations

## 4.1 Geometry

We first restrict ourselves to the simple Couette flow. We solve on the rectangular 2D domain with triangular elements. We consider all quantities to be two-dimensional. Boundary conditions are typical for the Couette flow: Velocity equal to zero on the bottom boundary and equal to non-zero value $v_{top}$ on the top boundary, representing a moving plate. The inflow and outflow have a zero Neumann boundary condition prescribed. The pressure is only given in one specific point somewhere in the domain. A reference value for the pressure was chosen to be zero. We can see the channel we used for calculations in the Figure 4.1. We will be calculating the apparent viscosity as defined in (3.1). We use the height of the canal equal to 1 m and we choose the $v_{top} = 2\,\mathrm{m/s}$. This setting of parameters leaves us with shear rate $\dot{\gamma} = 2s^{-1}$ according to the equation 3.2. Shear stress is in this simple case equal to the component of the Cauchy stress tensor $\mathbf{T}_{12}$. We will be able to show that we can measure the shear stress at an arbitrary point in the domain since it is constant in space.

## 4.2 Numerical methods

In this section, we briefly list the used numerical methods we use for solving the partial differential equations. We use Fenics, the open-source software. For more information about Fenics see [15]. In space, we use the continuous Galerkin finite element method with the linear elements for pressure and quadratic elements for other quantities, $\mathbf{v}$, $\mathbf{B}_{\kappa_{p(t)}}$ and $\mathbf{n}$. In time we use the implicit Euler scheme. For the solution of a system of linear equations, we use MUMPS solver. We iteratively solve the nonlinear equations using Newton iteration. The calculations are run on the Sňehurka computational cluster, available for the students of the Faculty of Mathematics and Physics at Charles University.

## 4.3 Shear flow results

### 4.3.1 Isotropic Oldroyd-B and Giesekus model

For comparison, we also simulate the Couette flow of the standard isotropic Oldroyd-B model (1.53) and the Giesekus model (1.59). We begin the simulation by setting $\mathbf{v} = 0\,\mathrm{m/s}, \mathbf{B}_{\kappa_{p(t)}} = \mathbf{I}, p = 0\,\mathrm{Pa}$ in the domain and by prescribing $v_{top} = 2\,\mathrm{m/s}$. We let the simulation reach the steady-state and plot the resulting velocity field. Since it was identical for the both models we can see the result in the Figure 4.2. Next we study the evolution of the apparent viscosity $\eta$. In the Figure 4.3 we can observe the typical overshot in the shear stress reflected in the apparent viscosity for the Giesekus model and a simple smooth transition to a steady-state for the Oldroyd-B model. The constants in the model are set to the following values

$$\mu = 1\,\mathrm{Pa}, \nu = 1\,\mathrm{Pa.\,s}, \nu_1 = 1\,\mathrm{Pa.\,s},$$

Figure 4.1: Computational domain. The boundaries and boundary conditions are marked.

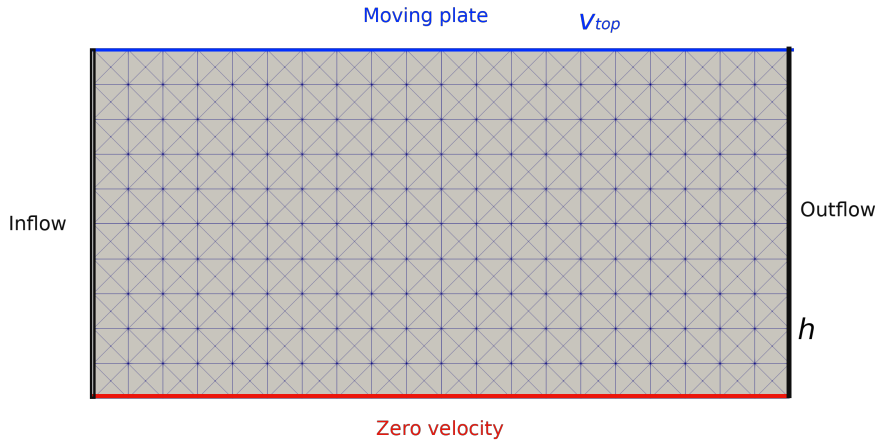


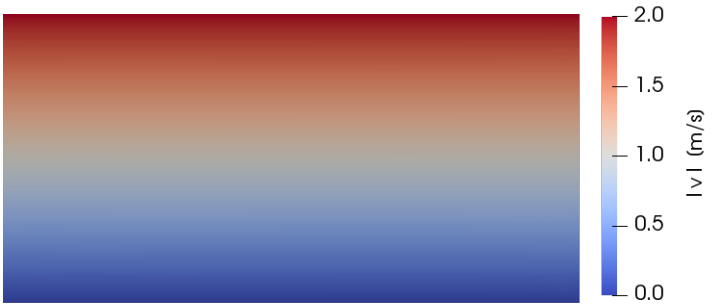


Figure 4.2: Velocity field for both Giesekus and Oldroyd-B model in the steady-state.

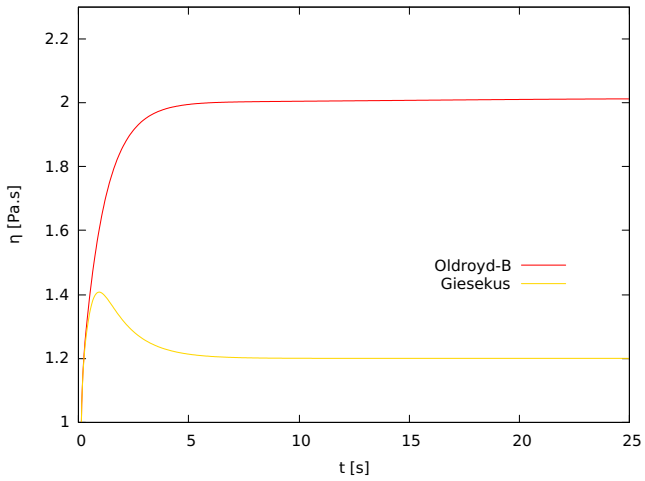


Figure 4.3: The apparent viscosity evolution for the isotropic models.

### 4.3.2 Anisotropic Oldroyd-B model

We would now like to investigate what an anisotropy brings into the solution. We are interested in the behavior of the vector $\mathbf{n}$. Specifically, we are going to study the evolution of the apparent viscosity $\eta$, the existence of a steady-state solution and the evolution of $\mathbf{n}$. We set the constants as follows

$$\mu = 1\,\mathrm{Pa}, \nu = 1\,\mathrm{Pa.\,s}, \nu_1 = 1\,\mathrm{Pa.\,s}, \nu_2 = 1\,\mathrm{Pa.\,s}, c = 1\,\mathrm{Pa}\,.$$

Using these settings we first plot the time evolution of $\mathbf{n}$. The results are in the Figure 4.4. We can see the effect of so-called tumbling. Vector $\mathbf{n}$ rotates in space and its movement seems to be periodic. We can see the plots of the apparent viscosity in the Figure 4.9 from the next Section compared to the other Oldroyd-B type models. As we discussed in the previous section, the tumbling-aligning transition is a studied phenomenon [16] [17]. We are therefore interested, whether our model can also show a flow-aligning behavior.

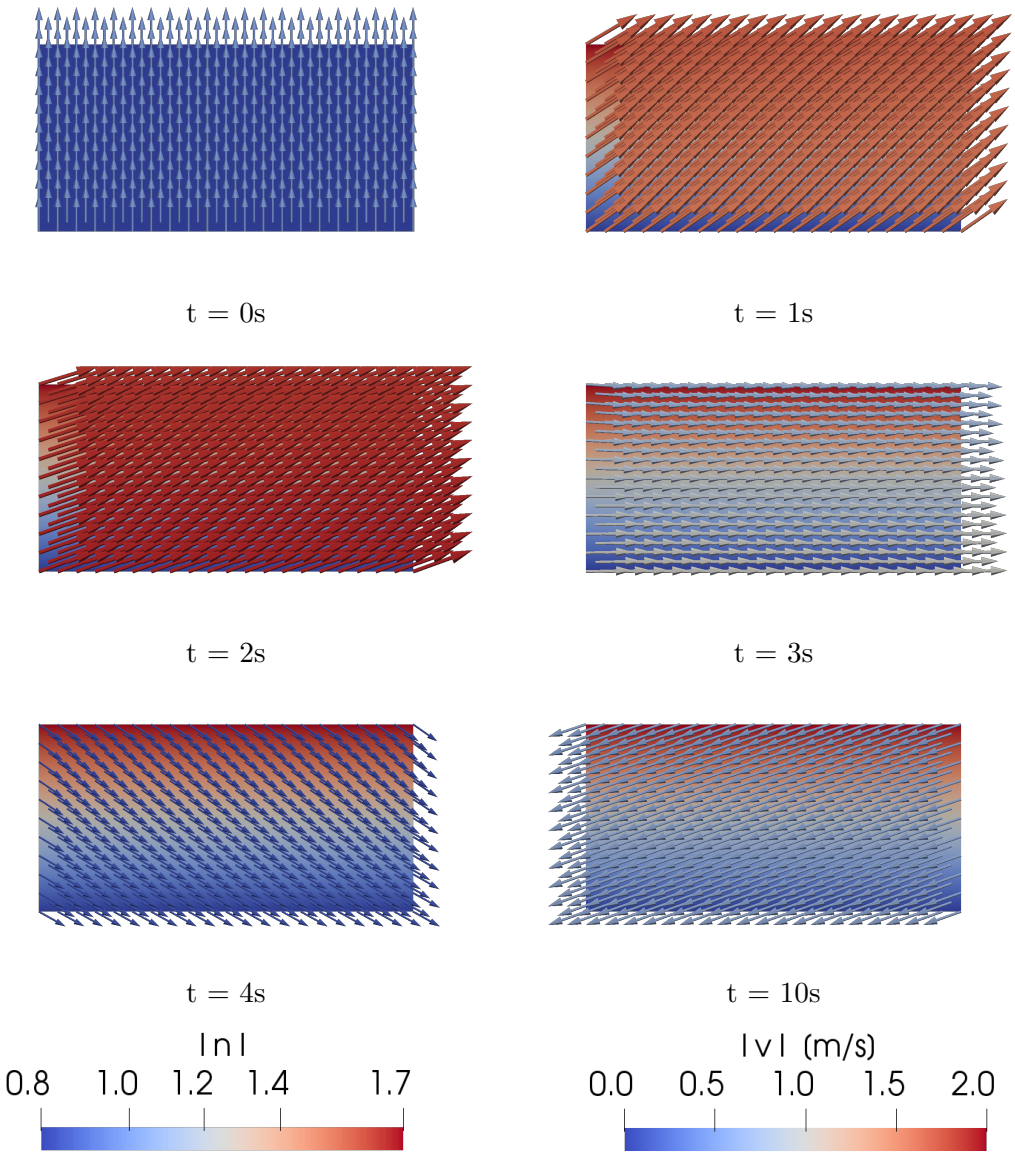


Figure 4.4: Anisotropic Oldroyd-B model. Time evolution of vector $\mathbf{n}$. For readers of the electronic version of the thesis, the animation is also available as mp4 file "AnisOldroydFig(4.4).mp4".

### 4.3.3 Model non-dissipative in $\mathbf{W}_{\kappa_{p(t)}}$

We will now investigate the behavior of model with $\nu_2 = 0\,\mathrm{Pa.\,s}$. For the equations see (2.61).

Keeping the other constants as follows

$$\mu = 1\,\mathrm{Pa}, \nu = 1\,\mathrm{Pa.\,s}, \nu_1 = 1\,\mathrm{Pa.\,s}, c = 1\,\mathrm{Pa}\,.$$

We yet again plot the same quantities as before. Now, however, we can clearly see from the Figure 4.5 and from the comparison 4.9 that there is a steady-state. Specifically, we can see flow alignment in this particular case. Since this model is basically the anisotropic Oldroyd-B model with a zero $\nu_2$ viscosity, we can expect

that there might be a value for $\nu_2$ that will be a border between tumbling and aligning behavior. After we introduce the remaining models and their behavior we will show that it is indeed the case.

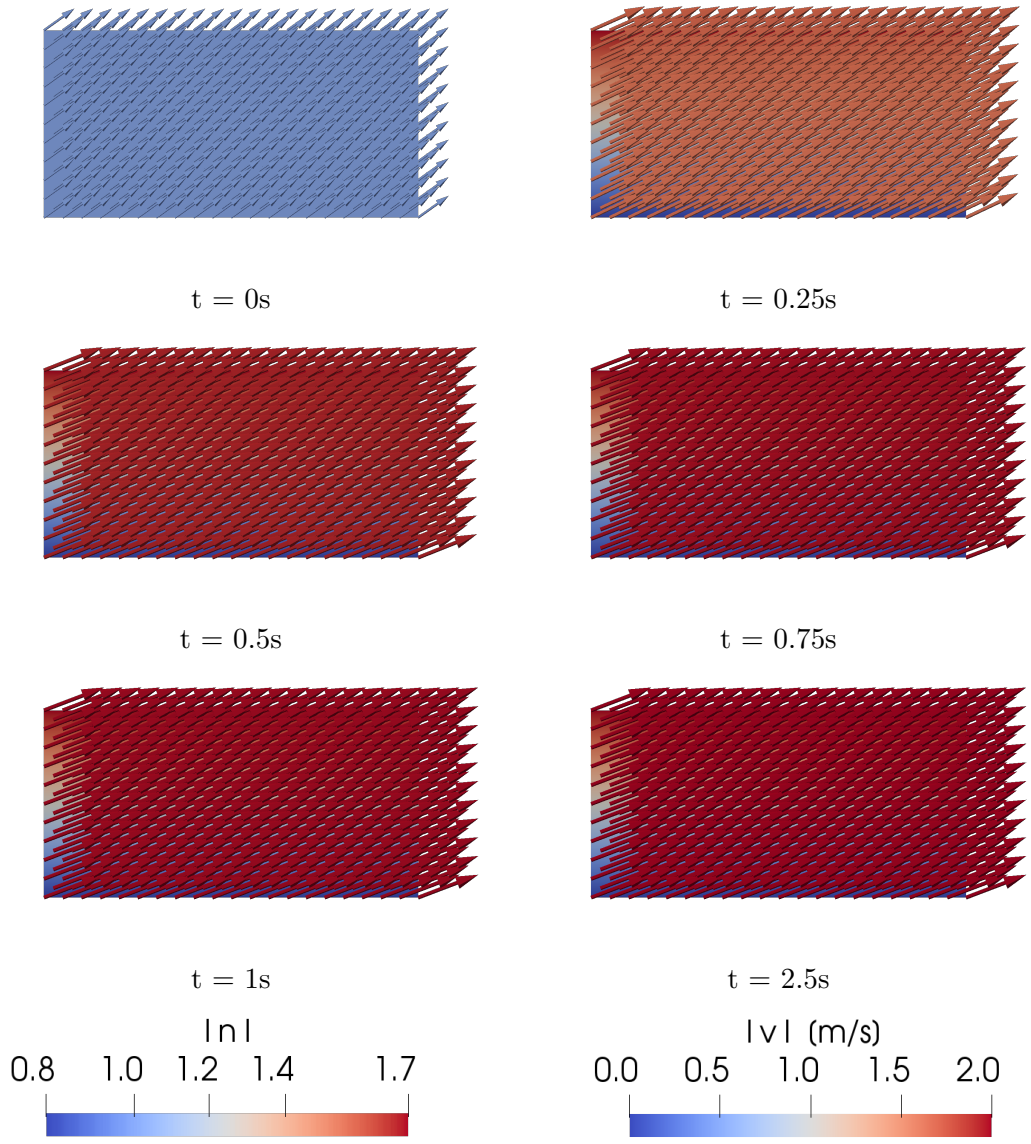


Figure 4.5: Model non-dissipative in $\mathbf{W}_{\kappa_{p(t)}}$. Time evolution of vector $\mathbf{n}$. Note there is a non-zero velocity field in the first timestep. It was necessary to start with values close to the steady-state, since this model is not as stable as models with $\nu_2 > 0$. For readers of the electronic version of the thesis, the animation is also available as mp4 file "NoDisiipFig(4.5).mp4".

### 4.3.4 Semi-analytical solution

The non-dissipative model is simple enough that we can, after some assumptions, calculate the result as a solution of algebraic equations. We will still be solving the equations numerically that is why we call it a semi-analytical solution but we will simplify the system in such a way that we will not need to solve the system

of partial differential equations. We assume that $\frac{\partial \mathbf{v}}{\partial x} = 0$ and $\frac{\partial \mathbf{v}}{\partial y} = \frac{v_{top}}{h}$. Next, we assume that in the steady-state state, variables $\mathbf{B}_{\kappa_{p(t)}}$, $p$ and $\mathbf{n}$ are constant in space. Those are indeed strong assumptions. We will, therefore, need to match the results calculated by this method with the finite element simulations for various parameter settings.

Before we start solving our system of algebraic equations, we shall first try to write them in the simplest possible form. Let us focus on the equation (2.60). We split $\mathbf{B}_{\kappa_{p(t)}}$ to $\mathbf{V}_{\kappa_{p(t)}}\mathbf{V}_{\kappa_{p(t)}}$ and multiply the equation by yet another $\mathbf{V}_{\kappa_{p(t)}}$

$$\mathbf{V}_{\kappa_{p(t)}}\mathbf{V}_{\kappa_{p(t)}}\mathbf{V}_{\kappa_{p(t)}}\mathbf{n}^* = \lambda\mathbf{V}_{\kappa_{p(t)}}\mathbf{n}^*, \tag{4.1}$$

that can be simplfied to

$$\mathbf{B}_{\kappa_{p(t)}}\mathbf{n} = \lambda\mathbf{n}. \tag{4.2}$$

The vector $\mathbf{n}$ is thus an eigenvector of the tensor $\mathbf{B}_{\kappa_{p(t)}}$ with an eigenvalue $\lambda$, as was $\mathbf{n}^*$. This shows that $\mathbf{n}^*$ and $\mathbf{n}$ are the same vectors except they may have a different size. In other words, when we find $\mathbf{n}^*$ we only need to find the size of $\mathbf{n}$. This enables us to change the variables we work with. Since $\mathbf{n}^*$ is a unit vector, it is in 2D fully specified by an angle

$$\mathbf{n}^* = \begin{pmatrix}\cos\alpha & \sin\alpha\end{pmatrix}. \tag{4.3}$$

We can therefore construct a vector $\mathbf{n}$ by

$$\mathbf{n} = \beta\mathbf{n}^*. \tag{4.4}$$

Using this we can now write the system of equations in a rather simplified way

$$\begin{aligned}\mu\Big(\mathbf{B}_{\kappa_{p(t)}} - \mathbf{I}\Big) + c\Gamma\Big(\mathbf{n}\otimes\mathbf{n}\Big) + \nu_1\overset{\triangledown}{\mathbf{B}}_{\kappa_{p(t)}} &= \mathbf{0},\\ \mathbf{B}_{\kappa_{p(t)}}\mathbf{n}^*\times\mathbf{n}^* &= \mathbf{0},\\ \mathbf{n}^*\cdot\mathbf{B}_{\kappa_{p(t)}}\mathbf{n}^* &= \beta\cdot\beta.\end{aligned}$$

Notice we are not solving for $\mathbf{v}$ since we have included its gradient in the assumptions and the only function satisfying our boundary conditions can be easily derived being

$$\mathbf{v} = \begin{pmatrix}y\cdot v_{top} & 0\end{pmatrix}, \tag{4.5}$$

while we denote $y$ a vertical coordinate and set it zero on the bottom plate and 1 on the top plate. These equations can now be solved and the results compared with the finite element simulations. We choose 4 different $v_{top}$ for which we calculate the tensor $\mathbf{B}_{\kappa_{p(t)}}$ and the vector $\mathbf{n}$ using both methods. We solve the algebraic equations using Wolfram Mathematica software FindRoot function. For finite elements simulations we use Fenics. We let the simulation run long enough until it is evident that no evolution is taking place and we have reached a steady state. In the table below we compare the semi-analytical solution (SA) with the results of finite elements method (FEM) simulation.

| $v_{top}$[m/s] | method | $(\mathbf{B}_{\kappa_{p(t)}})_{11}$ | $(\mathbf{B}_{\kappa_{p(t)}})_{12}$ | $(\mathbf{B}_{\kappa_{p(t)}})_{22}$ | $(\mathbf{n})_1$ | $(\mathbf{n})_2$ |
|---|---|---|---|---|---|---|
| 0.5 | SA | 1.095 | 0.2997 | 0.894 | 0.9293 | 0.6686 |
| 0.5 | FEM | 1.095 | 0.2997 | 0.894 | 0.9293 | 0.6686 |
| 1 | SA | 1.456 | 0.51 | 0.8247 | 1.152 | 0.6421 |
| 1 | FEM | 1.456 | 0.51 | 0.8247 | 1.152 | 0.6421 |
| 1.5 | SA | 1.982 | 0.6847 | 0.7801 | 1.379 | 0.6245 |
| 1.5 | FEM | 1.982 | 0.6847 | 0.7801 | 1.379 | 0.6245 |
| 2 | SA | 2.655 | 0.8454 | 0.7508 | 1.613 | 0.6127 |
| 2 | FEM | 2.655 | 0.8454 | 0.7508 | 1.613 | 0.6127 |

We can see that the simulation results are identical to the semi-analytical solution and that assumptions made were appropriate. Both $\mathbf{B}_{\kappa_{p(t)}}$ and $\mathbf{n}$ are indeed constant in space. The reason why we do not see any difference between both methods is that we used quadratic elements for unknown quantities. Constant functions are calculated exactly using quadratic elements.

### 4.3.5 Shear thinning like behavior

With the results from the previous chapter we now have a method that helps us to quickly and accurately explore the features of our model non-dissipative in $\mathbf{W}_{\kappa_{p(t)}}$. One interesting effect we can observe is shear thinning-like behavior. From the simulations, we have noticed that with a higher shear rate, the vector $\mathbf{n}$ gets more aligned with the flow. What happens to the shear stress is visible in the Figure 4.6. We can see that if we consider the steady-state, there is a clear nonlinear dependence of the shear stress on the velocity of the fluid. This

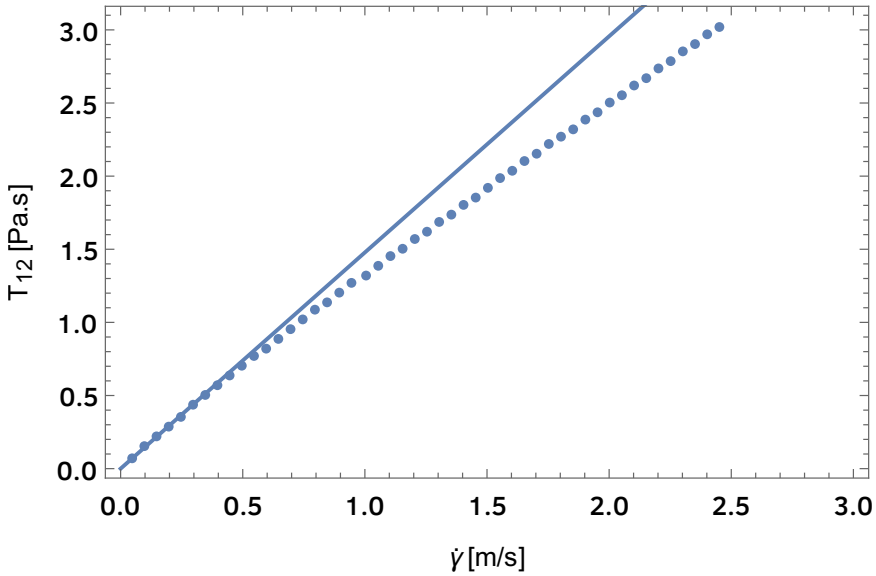


Figure 4.6: Dependence of the shear stress on the velocity of the fluid in the steady-state. The straight line is the linear fit of the first two points crossing zero, representing the fluid with no shear thinning behavior. The dotted line represents the calculated data.

is interesting since we did not use any model typically used for shear thinning. It follows directly from the character of anisotropy.

### 4.3.6 Anisotropic Giesekus model vith $\nu_1 = \nu_2$

The next model we would like to investigate is similar to the Giesekus model (2.39). We set $\nu_1 = \nu_2 = 1\,\mathrm{Pa.\,s}$. As we have seen, this simplifies the equations. We are interested in similar plots than before, namely, we would like to know if there exists a steady-state. From the Figures 4.7 and 4.10 we conclude there is no steady state and the vector $\mathbf{n}$ tumbles.

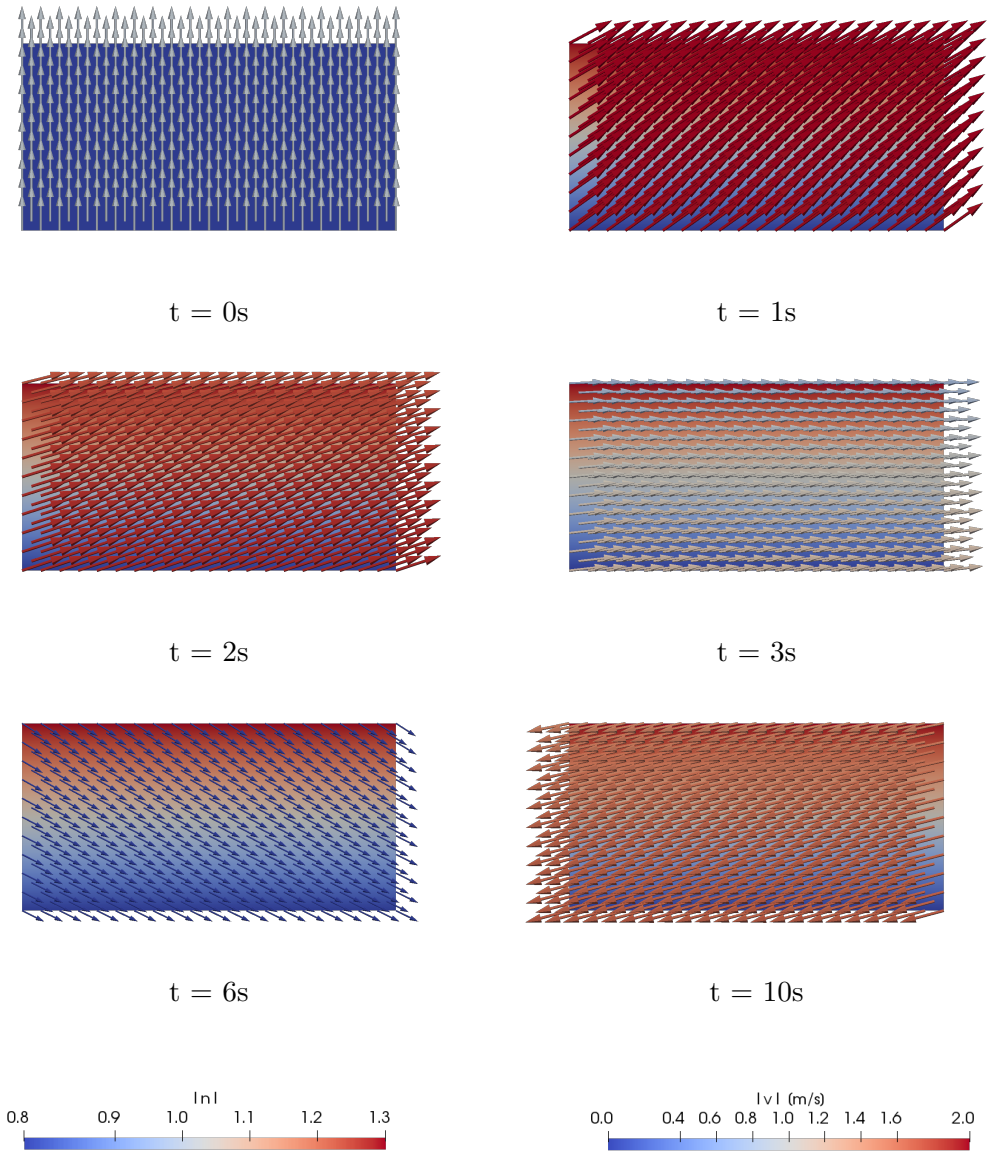


Figure 4.7: Model with $\nu_1 = \nu_2$. Time evolution of vector $\mathbf{n}$. For readers of the electronic version of the thesis, the animation is also available as mp4 file "EqViscFig(4.7).mp4".

### 4.3.7 Anisotropic Giesekus model with $\nu_2 = 0.1\,\mathrm{Pa.\,s}$

Finaly, we will show the evolution of the model with quadratic dissipation, while setting $\nu_2 = 0.1\,\mathrm{Pa.\,s}$ (2.76). We plot the evolution of vector $\mathbf{n}$ and the apparent

viscosity. This time, because of the low value of $\nu_2$, the vector aligns with the flow and the simulation reaches a steady-state. For evidence see the plots 4.8 and 4.10.

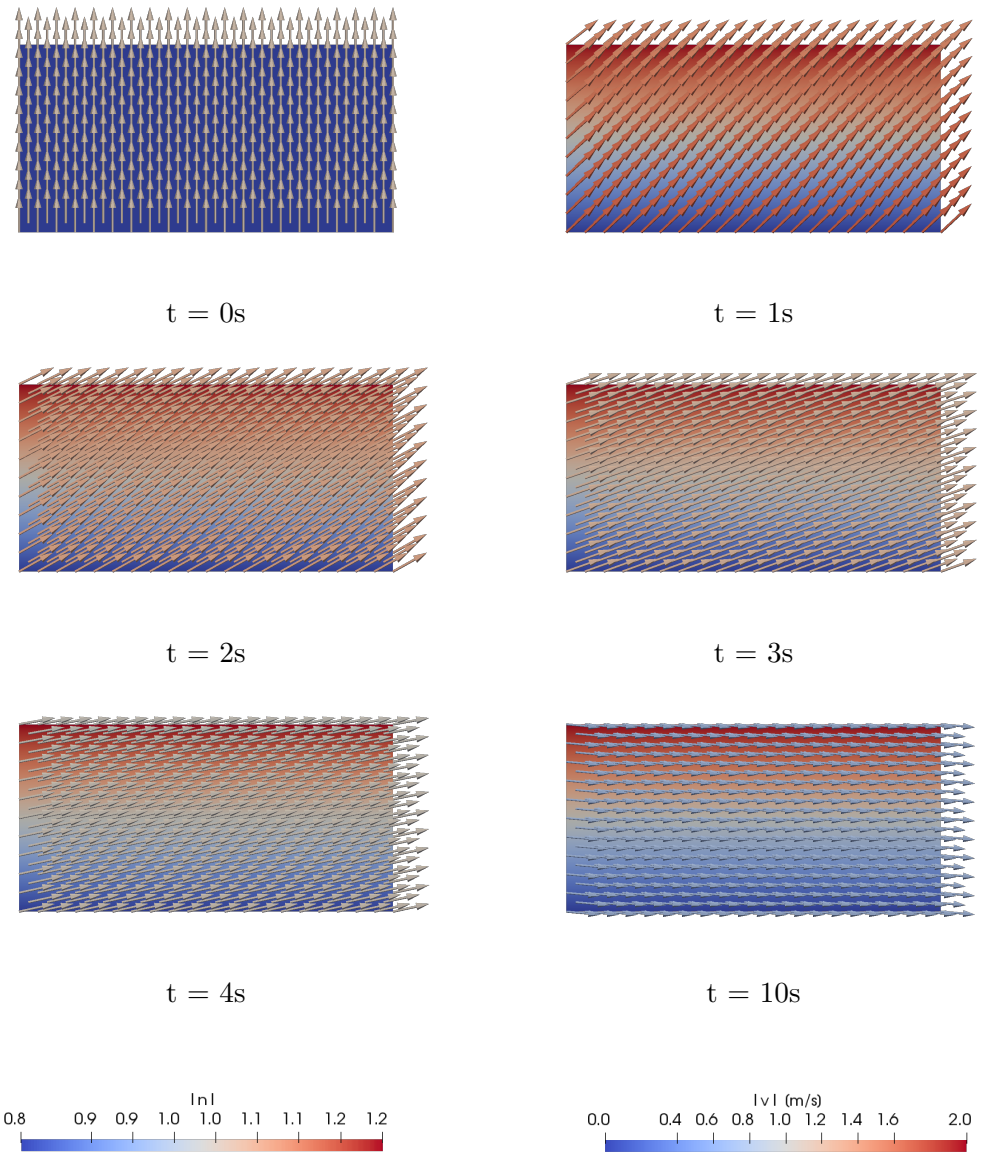


Figure 4.8: Model with quadratic dissipation $\nu_2 = 0.1$. Time evolution of vector **n**. For readers of the electronic version of the thesis, the animation is also available as an mp4 file "AnisGiesekusFig(4.8).mp4".

## 4.4 Comparison of shear stress evolution across the models.

We will compare the evolution of shear stress using different isotropic and anisotropic models and different settings of constants. This should give us an idea of how the anisotropy influences the flow. Moreover, Couette shear flow

is a realizable experiment. Therefore we can eventually compare the simulated results with experimental measurements and in the future find a material that our model describes. We will focus firstly on the Oldroyd-B type models.

### 4.4.1 Oldroyd-B type models

In this class, we plot the apparent viscosity for three models. Isotropic Oldroyd-B model, anisotropic Oldroyd-B model, and model with no dissipation in $\mathbf{W}_{\kappa_{p(t)}}$. These models, as mentioned during their derivation, are similar since the evolution equation for $\mathbf{B}_{\kappa_{p(t)}}$ is in $\mathbf{B}_{\kappa_{p(t)}}$ linear. For simplicity, we will keep all the constants set to 1. From the previous section, we know that for the isotropic Oldroyd-B model and model with no dissipation in $\mathbf{W}_{\kappa_{p(t)}}$ we have a steady-state solution for studied flow. Anisotropic Oldroyd-B model has no steady-state solution because the vector $\mathbf{n}$ keeps spinning. How the shear stress behaves can be seen in the Figure 4.9.

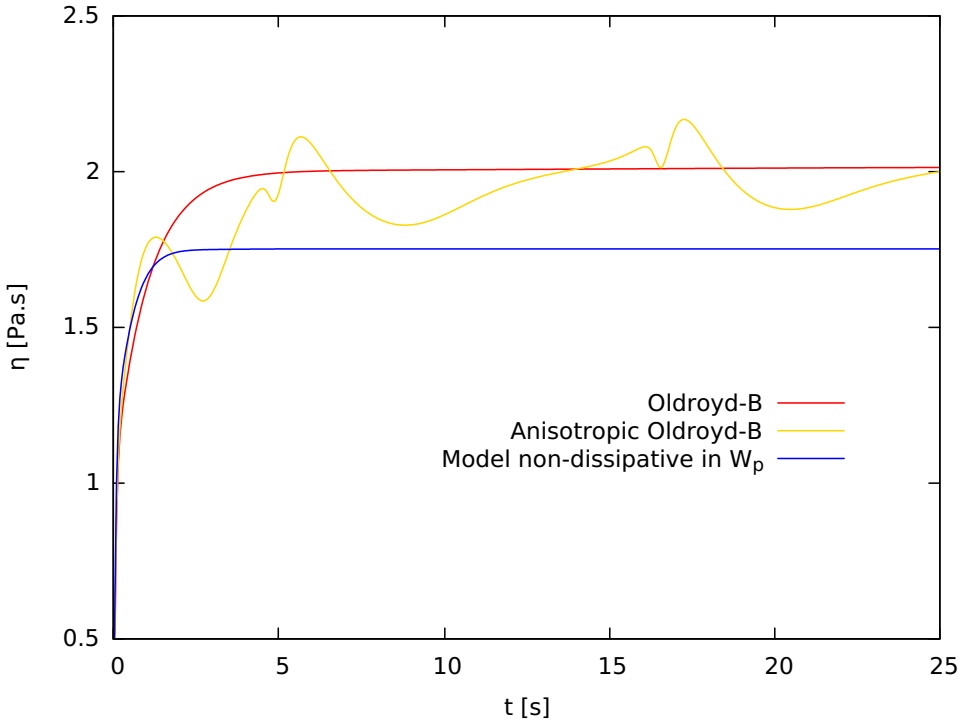


Figure 4.9: Comparison of shear stress evolution in Oldroyd-B type models.

### 4.4.2 Giesekus type models

One of the anisotropic models is similar to Giesekus isotropic model. Model with $\nu_1 = \nu_2$ can be simplified as described in the Section 2.4.4. This leads to the model quadratic in $\mathbf{B}_{\kappa_{p(t)}}$. The model has no steady-state for our usual setting of constants to 1. We can see the shear stress evolution compared to the pure isotropic model in the Figure 4.10

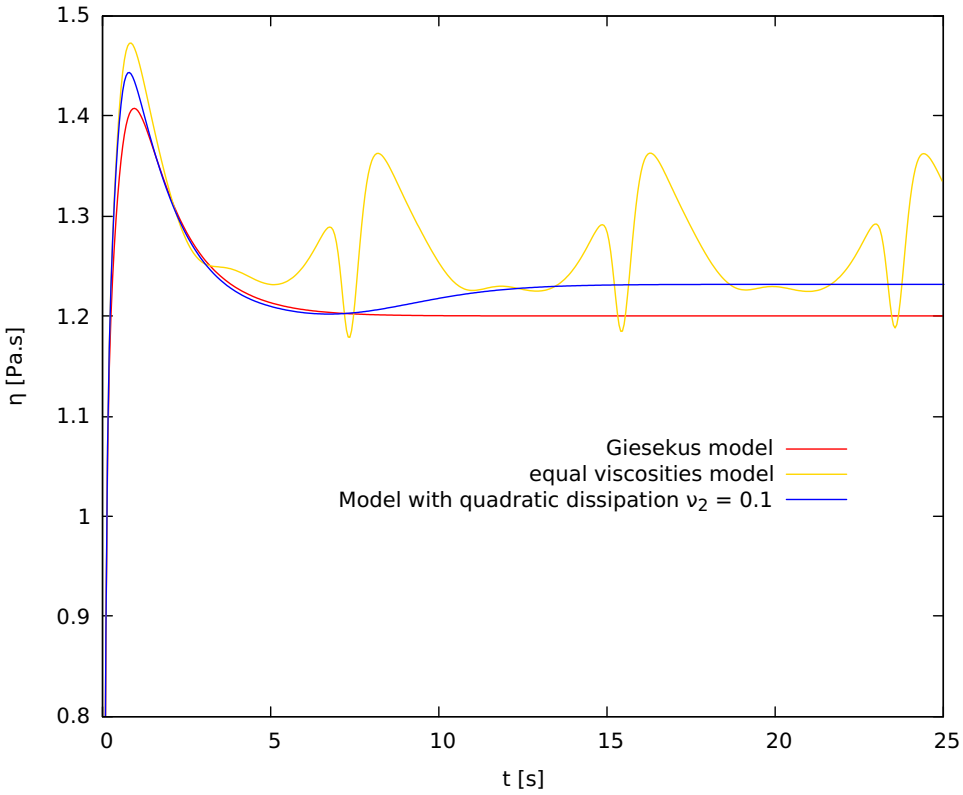


Figure 4.10: Comparision of shear stress evolution in Giesekus type models.

## 4.5 Influence of $\nu_2$

In this section, we will investigate various constants settings. We will stop using every constant equal to 1 and investigate if there, for example, exists a steady state if we change one of the viscosities or study the influence on the relaxation time of a model if a steady state is present.

### 4.5.1 Anisotropic Oldroyd-B model

We would like to study the influence of different settings of $\nu_2$. We expect different speeds of rotations or even the simulation converging to a steady state. First, we select a broad range of parameters. The results for the shear stress evolution can be seen in the Figure 4.11.

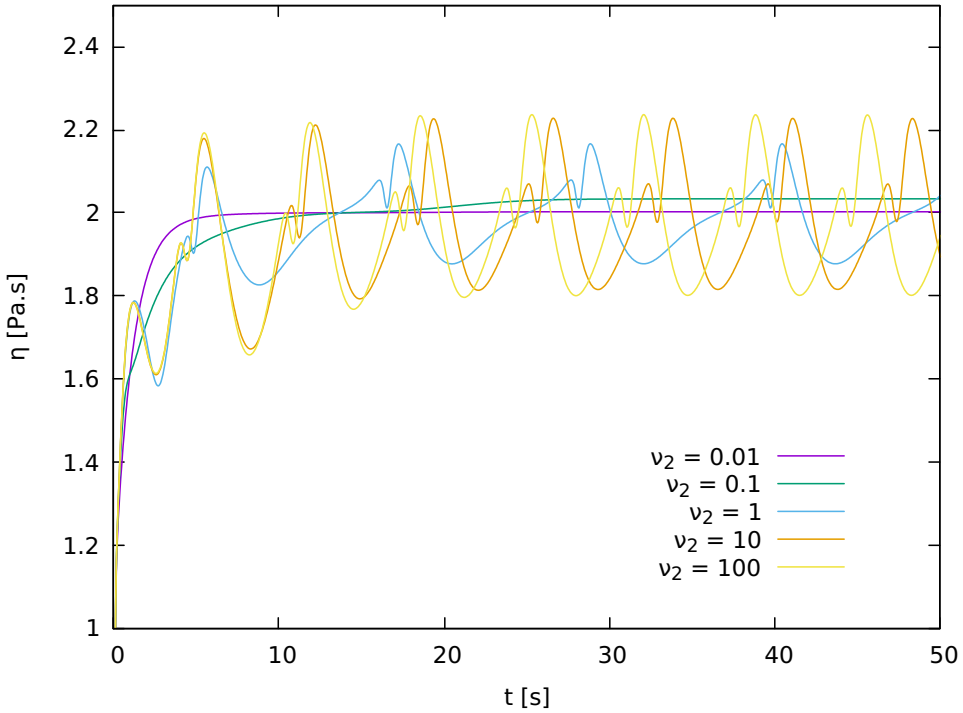


Figure 4.11: Using only anisotropic Oldroyd-B model we look at various setting of $\nu_2$. We can see the shift in behavior from tumbling state when viscosity is high to steady state when $\nu_2$ is low. The rotation is also faster for higher values of $\nu_2$.

Next we look more closely to what happens when we investigate tumbling - steady transition at $\nu_2 \approx 0.19\,\mathrm{Pa.\,s}$. The results can be seen in the Figure 4.12

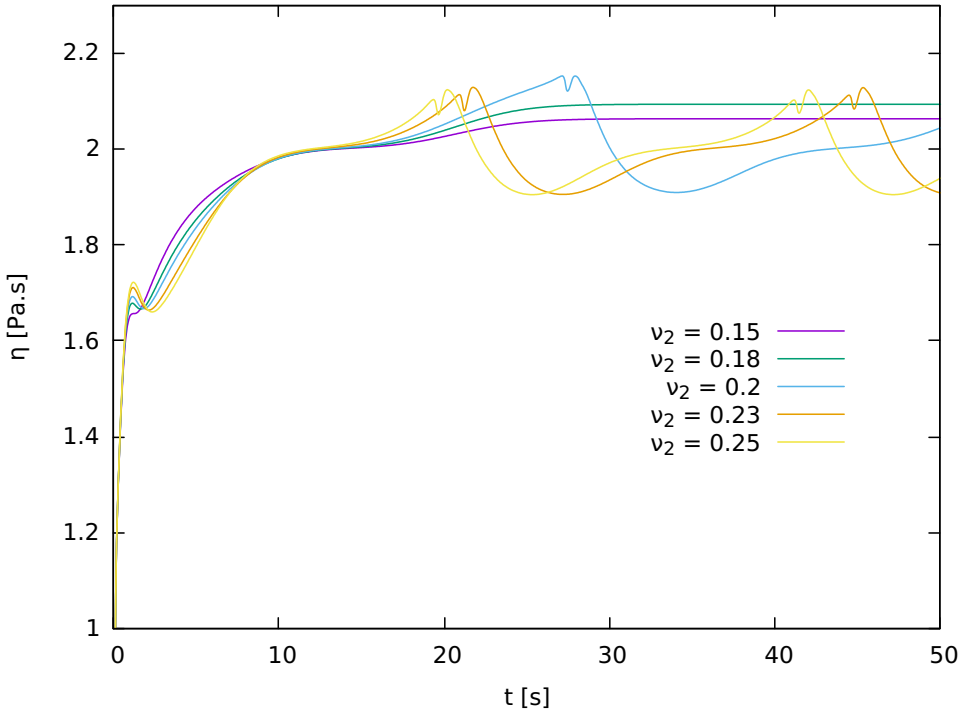


Figure 4.12: We focus on the samller range $\nu_2 \in \{0.15$ Pa.s, 0.18 Pa.s, 0.2 Pa.s, 0.23 Pa.s, 0.25 Pa.s$\}$ . We see the transition behavior from tubmling to the steady-state.

## 4.6 3D Simulation

We will now look at the results from the simulation inspired by the experiment described in the Section 3.1.4. We use the model with quadratic dissipation setting $\nu_1 = \nu_2$. This model is described by the equations (2.76). We use tetrahedral elements and the same numerical methods as for the 2D problem. We plot the snapshots of vector field $\mathbf{n}$ in the Figure 4.13 and then plot the integrated shear stress divided by the integrated shear rate. We denote this quantity as $\overline{\eta}$.

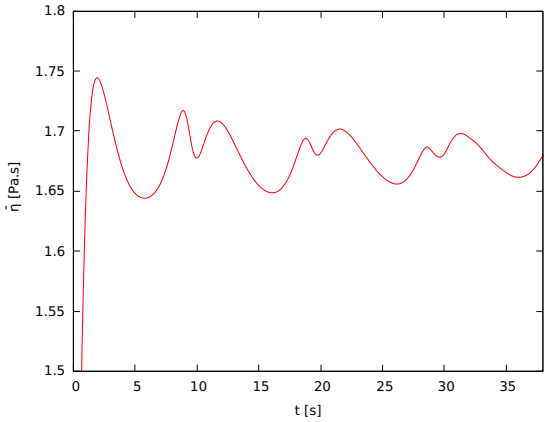


Figure 4.14: Plot of $\overline{\eta}$ for 3D simulation using model 2.4.4. Previously defined $\overline{\eta}$ is plotted versus time, since shear would not be constant for all points.

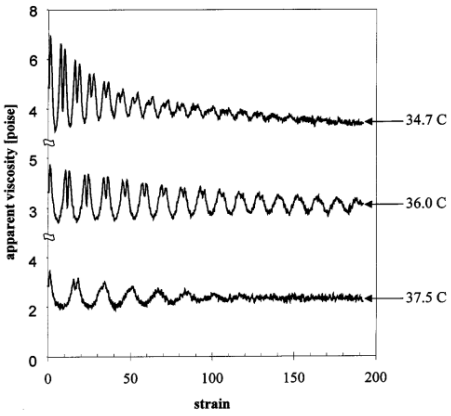


Figure 4.15: Figure 11 from the article [6]. Plot of the apparent viscosity for a liquid crystal mixture and three temperatures obtained from the experiment using cone and plate rheometer.

We would now like to compare the plot of $\overline{\eta}$ with the experimental results obtained for the apparent viscosity of a liquid crystal in the article [14] (see Figures 4.14 and 4.15). We may notice there are some features similar. Firstly, we see that both curves have periodic behavior over time. The characteristic drop around the maximum of each period is present in the simulation as well as in the measurement. The last important feature we would like to discuss is the decreasing amplitude of the periods. In our model, it has a clear meaning. We are integrating the shear stress and we may notice in the snapshots that the vectors tend to desynchronize. This way the position of the vector $\mathbf{n}$ is more and more random and the amplitude of the average gets lower. In the experimental data, the decrease in the amplitude is also present. We suspect this may be caused by the cone not fully touching the plate in the rheometer. This would create the non-uniform shear rate since the equation (3.1) would not be entirely correct. Non-uniform shear rate leads to the same effect as in our plate and plate simulation. There may also be other reasons why the amplitude decreases after a certain time interval like the heating of the liquid crystal or imperfections in the mixture preparation.

Even though we did not fit the model, nor used exactly the same geometry in the simulation, we consider the qualitative agreement in the results interesting and worth further research. The plate and plate geometry may be at the end relevant since it probably captures the imperfection in the homogenous orientation of anisotropy after a period of time. Cone and plate simulation can be developed after we explore how to stabilize the model in more complex geometries.

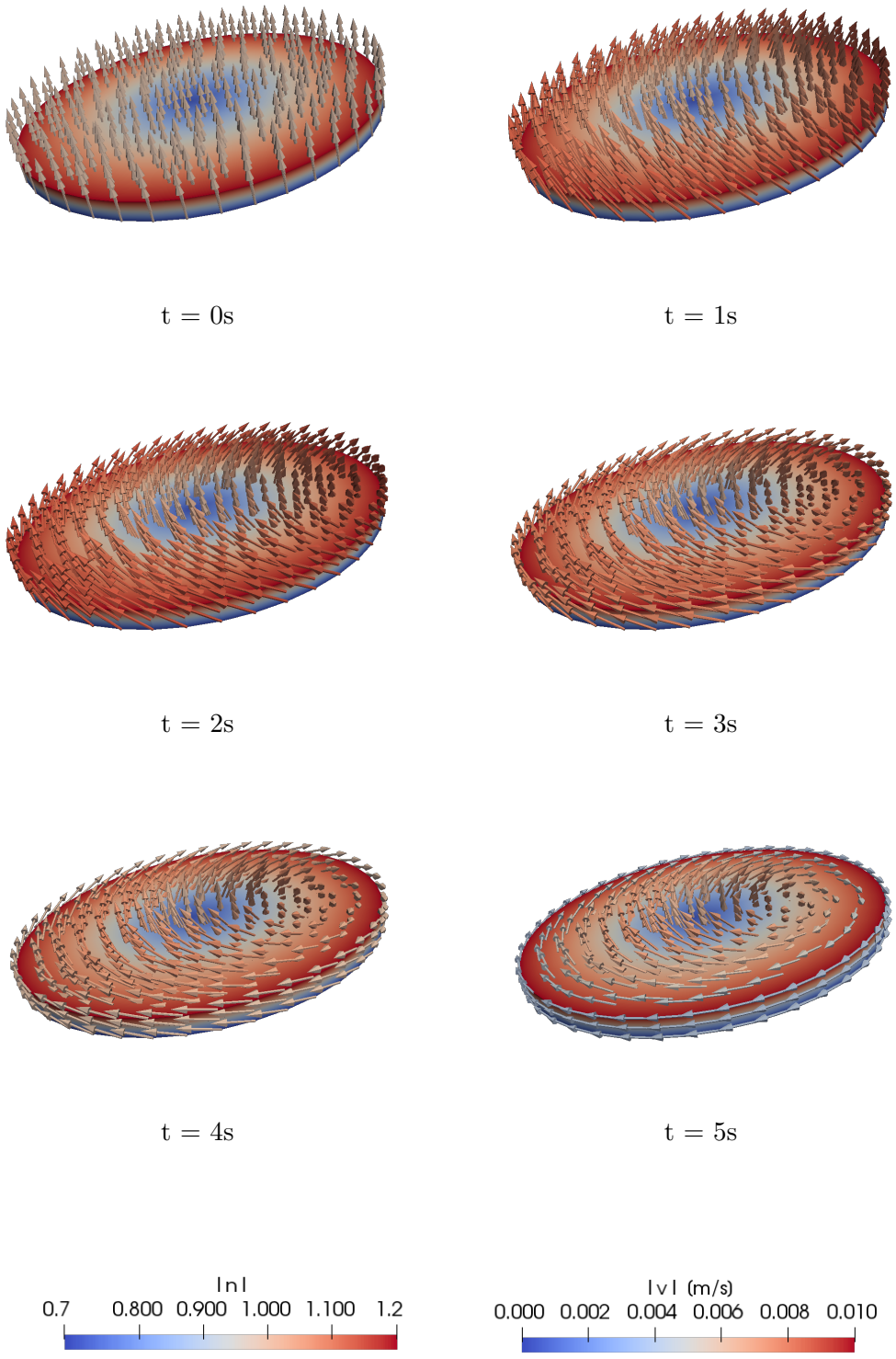


Figure 4.13: Model with $\nu_1 = \nu_2$. Time evolution of vector $\mathbf{n}$ for 3D simulation. For readers of the electronic version of this thesis, the animation is available as mp4 file "3DsimFig(4.13).mp4".

# Conclusion

In this thesis we introduced new thermodynamicaly consistent models of an anisotropic viscoelastic fluids. In the first chapter, we introduced important quantities and relations and extended them further including the anisotropy. We derived four models as an example of how to approach and work with the framework developed. We put the models into two categories depending on whether they have a linear or quadratic equation for $\mathbf{B}_{\kappa_{p(t)}}$ calling them Oldroyd-B and Giesekus type respectively. The comparison of isotropic against anisotropic models was also done showing interesting patterns such as tumbling/aligning of the vector $\mathbf{n}$ or different speed of rotation deppending on the angle between $\mathbf{n}$ and velocity vector. Finally, we tried to see if the model developed using only very basic assumptions and principles can in some way capture the bahavior of a liquid crystal. We simulated the geometry similar to the cone and plate rheometer used for measurements in the article [14] and qualitatively compared the results. The resemblance of the key curve patterns between the simulated and experimental data was rather interesting.

There is a lot of potential for further work to be done that can lead to interesting results. We believe that tumbling and aligning transition can be investigated analytically and possibly a critical value for $\nu_2$ can be determined. For all calculations, we used a continuous Galerkin finite element method. Since the vector field $\mathbf{n}$ can be discontinuous in a general case, discontinuous numerical methods for solving partial differential equations could lead to more stable and robust solvers for liquid crystals.

In the future, the expansion of free energy including the terms with $\nabla\mathbf{n}$ should be considered, representing the so-called distortion free energy typically present in certain classes of liquid crystals.

# Bibliography


[1] R. Edgeworth, B. Dalton, and T. Parnell. The pitch drop experiment. *European Journal of Physics - EUR J PHYS*, 5:198–200, 1984.

[2] J. G. Oldroyd and A.H. Wilson. On the formulation of rheological equations of state. *Proceedings of the Royal Society of London. Series A. Mathematical and Physical Sciences*, 200(1063):523–541, 1950.

[3] H. Giesekus. A simple constitutive equation for polymer fluids based on the concept of deformation-dependent tensorial mobility. *Journal of Non-Newtonian Fluid Mechanics*, 11(1):69 – 109, 1982.

[4] K.R. Rajagopal. Multiple configurations in continuum mechanics. *Reports of the institute for computational and applied mechanics*, 6, 1995.

[5] K.R. Rajagopal and A.R. Srinivasa. A thermodynamic frame work for rate type fluid models. *Journal of Non-Newtonian Fluid Mechanics*, 88:207–227, 2000.

[6] K.R. Rajagopal and A.R. Srinivasa. On the thermomechanics of materials that have multiple natural configurations part i: Viscoelasticity and classical plasticity. *Zeitschrift fur Angewandte Mathematik und Physik*, 55:861–893, 2004.

[7] J. Málek, K.R. Rajagopal, and K. Tůma. On a variant of the maxwell and oldroyd-b models within the context of a thermodynamic basis. *International Journal of Non-Linear Mechanics*, 76:42 – 47, 2015.

[8] K.R. Rajagopal and A.R Srinivasa. Modeling anisotropic fluids within the framework of bodies with multiple natural configurations. *J. Non-Newtonian Fluid Mech*, 99:109–124, 2001.

[9] H.B. Callen. *Thermodynamics and an Introduction to Thermostatistics*. Wiley, 1985.

[10] K.R. Rajagopal and A.R. Srinivasa. On thermomechanical restrictions of continua. *Proceedings of the Royal Society A: Mathematical, Physical and Engineering Sciences*, 1111:631–651, 2002.

[11] F. C. Frank. I. liquid crystals. on the theory of liquid crystals. *Discuss. Faraday Soc.*, 25:19–28, 1958.

[12] F.M. Leslie. Some constitutive equations for liquid crystals. *Archive for Rational Mechanics and Analysis*, 28(4):265–283, 1968.

[13] P.G. de Gennes and J. Prost. *The Physics of Liquid Crystals*. International Series of Monogr. Clarendon Press, 1993.

[14] L. Leal, R. Larson, and D. Ternet. Flow-aligning and tumbling in small-molecule liquid crystals: Pure components and mixtures. *Rheologica Acta*, 38:1–2, 1999.

[15] A. Logg, K.A. Mardal, G.N. Wells, et al. *Automated Solution of Differential Equations by the Finite Element Method*. Springer, 2012.

[16] P. A. Campos and A. F. Martins. The director tumbling-alignment transition in shear flows of nematic liquid crystal polymers, modelled by continuum theory. In I. Emri, editor, *Progress and Trends in Rheology V*, pages 216–217, Heidelberg, 1998. Steinkopff.

[17] A.D. Rey. *Field-Induced Orientation in Nematic Liquid Crystals.* PhD thesis, UNIVERSITY OF CALIFORNIA, BERKELEY., 1988.